Talanta Open 7 (2023) 100191

Contents lists available at ScienceDirect

Talanta Open

journal homepage: www.sciencedirect.com/journal/talanta-open

A critical review of the two-temperature theory and the derivation of matrix elements. High field ion mobility and energy calculation for all-atom structures in light gases using a 12-6-4 potential

Viraj D. Gandhi [a,b], Leyan Hua [a], Xuemeng Chen [a,c], Mohsen Latif [a,1], Carlos Larriba-Andaluz [a,*]

[a] Department of Mechanical & Energy Engineering, Indiana University – Purdue University Indianapolis, SL 260, 723W. Michigan Street, Indianapolis, IN 46202, USA
[b] Department of Mechanical Engineering, Purdue University, West Lafayette, USA
[c] Faculty of Science and Technology, University of Tartu, Tartu, Estonia

ARTICLE INFO

Keywords:
Two-temperature theory
Ion-mobility
High-field
Higher-order approximation
Collision cross section

ABSTRACT

Ion mobility has become a ubiquitous tool in many aspects of Analytical Chemistry due to its ability to separate compounds in the gas phase prior to feeding them to a Mass Spectrometer. To understand how this complex separation occurs, it is necessary to thoroughly explain the ion-gas interaction. In particular, this manuscript aims to describe the physics behind the collisions at high fields using the two-temperature approximation. The two-temperature theory has been recently employed to describe the mobility of polyatomic ions quite successfully and thus a proper account is warranted. A concise description is provided along with rigorous mathematical arguments behind its success at predicting the ion's drift velocity. Moreover, a thorough procedure for obtaining the equations (including the matrix elements) for higher-order mobility approximations is also provided with high detail, making this work suitable for beginners and experts in ion mobility. In particular, a discussion is brought forth on the choice of the base temperature and its relation to both the effective temperature and the drift velocity of the ion. A comparison between a 12-6-4 potential and the Maxwell model is made, pointing at the possible errors of using the Maxwell model for low- and high-field calculations. Using our in-house algorithm IMoS, successive approximations up to the fourth are tested against previous ones and against experimental results, showing both, asymptotic convergence, as well as a good agreement for monoatomic gases and small ions.

1. Introduction

Ion Mobility Spectrometry (IMS) is maturing at an enormous rate, showing that gas phase separations are becoming key in analyte characterization [1–4]. This recognition is not unfounded as the technique has been shown to separate compounds such as isomers and isotopomers that cannot be resolved by Mass Spectrometry alone (MS) [5–7]. As instruments improve their resolution, some separations are no longer well-understood by the concurrent theory and new avenues must be explored and reasoned, while older ones may need to be dusted and improved [8,9].

This work falls on the latter aspect, where the main goal is to describe how and why the two-temperature theory is an acceptable approach, showing how to obtain the matrix elements (up to the fourth approximation) regardless of the orthogonal functions that are used. This laborious effort will ease the calculation of collision integrals for other theories and orthogonal sets (e.g., Hermite polynomials and the three-temperature theory). A major reason is that full derivations of the elements have never been shown in detail and are only tabulated to the second approximation [10,11]. A variation of the truncation method brought forth by Mason and Viehland is also shown as well as a novel way of obtaining the ion's energy that greatly speeds up the calculation process.

We have previously shown that the two-temperature theory is more than capable of describing the high-field (and or temperature) behaviour of all-atom models in light gases [1]. The results show good behaviour even for the first approximation although improvements are observed when higher-order approximations are included (up to the fourth). The

* Corresponding author.
E-mail address: clarriba@iupui.edu (C. Larriba-Andaluz).
[1] linkedin.com/in/mohsen-latif/

https://doi.org/10.1016/j.talo.2023.100191

Available online 19 February 2023

main reason for the success of the two-temperature theory relies on two interrelated features. The first one considers that the ion's velocity distribution is a function of a temperature which varies with E/n and is different from that of the gas while the second one, a consequence of the first, is that all higher-order terms are bounded (something not possible in the one temperature theory) [9] so any approximation is valid at all fields. The assumptions are that the distribution is still nearly Gaussian even at high fields and that the ion has been accelerated to a constant drift velocity and has been heated to an effective temperature due to collisions with the gas at high relative speeds. [12]

The manuscript is divided into two parts. First, an introduction to the theory together with an explanation of the mobility calculation and accompanied by a description of how to obtain the matrix elements (the full calculation of all necessary elements is provided in the supplementary information) as well as how to obtain the ion's energy (or the relation between field over gas concentration (E/n) and the ion's temperature). This is followed by a discussion on the collision integrals for hard spheres and 12-6-4 potentials and how their ratios vary from the normally accepted Maxwell model. The article also provides a comparison between the different approximations as a function of the electric field for different mass ratios.

2. Theoretical description

To introduce the concept of the two-temperature theory, one should start by describing the series of approximations that must be done for the Boltzmann equation employed to be valid [13]. The first and most important is that the ion is small enough that it does not perturb the gas. Other approximations are that collisions are assumed to be elastic, that the gas distribution may be considered Maxwellian (independent of position and time and fixed at a given temperature), and that the number-density of the ions, N, is small enough that ion-ion interactions may be neglected. Under these assumptions, the Boltzmann equation for an ion's velocity distribution $F(z_i)$ in the presence of a neutral gas with distribution $(f(c_i))$ is given by Viehland and Mason [11,14–16]:

$$\frac{\partial F}{\partial t}+z_j\frac{\partial F}{\partial x_j}+a_j\frac{\partial F}{\partial z_j}=n\int\int\int(f'F'-fF)gbdbd\epsilon dc_i \tag{1}$$

In the equation above, n is the number-density of gas, z_i and c_i are the ion and gas velocities respectively while $g_i=z_i-c_i$ is the relative velocity, b is the impact parameter (distance between the ion and gas in the transversal direction to the ion's drift), ϵ is the intrinsic rotation angle and x_i, a_i and t are position, acceleration, and time. In Eq. (1), it is initially assumed that the ion's velocity distribution depends on position and time and that the acceleration is general. The term on the right hand side corresponds to the collision term, where only interactions between gas and ion are accounted for. The collision term represents the replenishment (coming from prime sources) and extinguishment of ions of class velocity z_i through collisions with gas molecule velocities between c_i and c_i+dc_i (where $dc_i=dc_1dc_2dc_3$). We shall simplify the equation even further by assuming that the distribution does not depend on position x_i or time t and that the acceleration a_j only depends on a constant field value E (relaxation effects are neglected) in the direction of ion movement $z_1=w$. Under such conditions, the equation becomes more manageable [17,18]

$$\frac{eE}{Mn}\frac{\partial F}{\partial w}=\int\int\int(f'F'-fF)gbdbd\epsilon dc_i \tag{1b}$$

where, e is the elemental charge (assuming the ion is singly charged) and M is the mass of the ion. Despite the simplifications, the equation is still difficult to solve even when the gas and the ion are considered spherical atoms [17,18]. The main reason is that the term $(f'F'-fF)$ is dependant on the ion-gas interaction. In general, an assumption generally relies on choosing a solution dependant on orthogonal polynomials as [19]:

$$F=F^{(0)}\sum_p a_p\phi_p=\left(\frac{M}{2\pi kT_b}\right)^{\frac{3}{2}}e^{-\frac{M(z_i)^2}{2kT_b}}\sum_p a_p\phi_p \tag{2}$$

where ϕ_p are orthogonal functions, a_p are unknown coefficients and $F^{(0)}$ is the basis or zeroth function chosen for the two-temperature theory. k is the Boltzmann's constant and T_b is a temperature-like parameter that needs to be defined (generally called the base temperature). It is normally equated to the ion's lab reference of frame temperature (see Eq. (17) for an analytical expression and further explanation) which includes the kinetic energy from the field and heating due to the collisions with the gas, both effects contributing to the ion's temperature above that of the equilibrium gas temperature T. Due to the addition of the kinetic energy, T_b is not a thermodynamic temperature as such, but more akin to a dynamic temperature. Note that the choice of $F^{(0)}$ is important. If the choice of the basis function was exactly F, then the sum of orthogonal functions would be one, not requiring one to obtain the a_p coefficients. A close choice would allow the least number of coefficients to be calculated in order to get a solution [20–22].

Even with Eq. (2), solving Eq. (1b) is not possible in general [23–25]. An option is to resort to calculating moments of F. This is obtained by multiplying Eq. (1b) by a function of the ion's velocity $\psi_{lm}^{(r)}$ and integrating over all possible velocities z_i, i.e., $\psi_{lm}^{(r)}Av=\int F\psi_{lm}^{(r)}dz_i$, obtaining average quantities (moments) and leading to [25]:

$$\frac{eE}{Mn}\left\langle\frac{\partial\psi_{lm}^{(r)}}{\partial w}\right\rangle_{Av}=<\mathscr{J}\psi_{lm}^{(r)}>_{Av}, \tag{3}$$

where, $\mathscr{J}$ is the operator given by:

$$\mathscr{J}\psi_{lm}^{(r)}=\int\int\int f\left(\psi_{lm}^{(r)}-\psi_{lm}^{(r)'}\right)gbdbd\epsilon dc_i \tag{4}$$

To arrive at Eq. (3) from (1b), integration by parts and the inverse collision property have been used (refer to the supplementary information of this paper or Eqs. (B.4)–(B.9) in Ref. [9] or Ref. [26] to see the calculation) as well as the use of the basis function approximation (Eq. (2)). A solution to Eq. (3) may be obtained by choosing appropriate orthogonal functions $\psi_{lm}^{(r)}$, and where the practicality of the solution heavily relies on how close the orthogonal functions are to eigenfunctions of the operator $\mathscr{J}$. Commonly employed for the two-temperature theory are the Burnett spherical polar functions given by Spalding [27,28]:

$$\psi_{lm}^{(r)}=\left(\frac{M|z|^2}{2kT_b}\right)^{\frac{l}{2}}P_l\left(\frac{w}{|z|}\right)S_{l+\frac{1}{2}}^{(r)}\left(\frac{M|z|^2}{2kT_b}\right)e^{im\phi} \tag{5}$$

Here P_l are the Legendre polynomials and $S_{l+\frac{1}{2}}^{(r)}$ are the Sonine (associated Laguerre) polynomials. The Burnett functions happen to be the eigenfunctions of the operator $\mathscr{J}$ for the Maxwell Model, and hence a suitable candidate [29]. The Maxwell model is a simple potential interaction that corresponds to a repulsion interaction of r^{-4} (showcased in Fig. 1). Its importance relies on the fact that its result can be computed analytically, (due to its eigenvalue properties) and hence becomes an important point of reference. Note that T_b is the same temperature used in the basis function in order to utilize the integral superposition method [30,31]. The Burnett functions are orthogonal to the inner product [16]:

$$\left(\psi_p,\psi_{p'}\right)=\int e^{-\frac{M(z_i)^2}{2kT_b}}\psi_p^{\dagger}\psi_{p'}dz_i=\int F^{(0)}\psi_p^{\dagger}\psi_{p'}dz_i=A_p\delta_{pp'} \tag{6}$$

With † describing complex conjugation and where the basis function $F^{(0)}$ appears as the required weight. For two functions formed using Eq. (5), the inner product yields [11,32]:

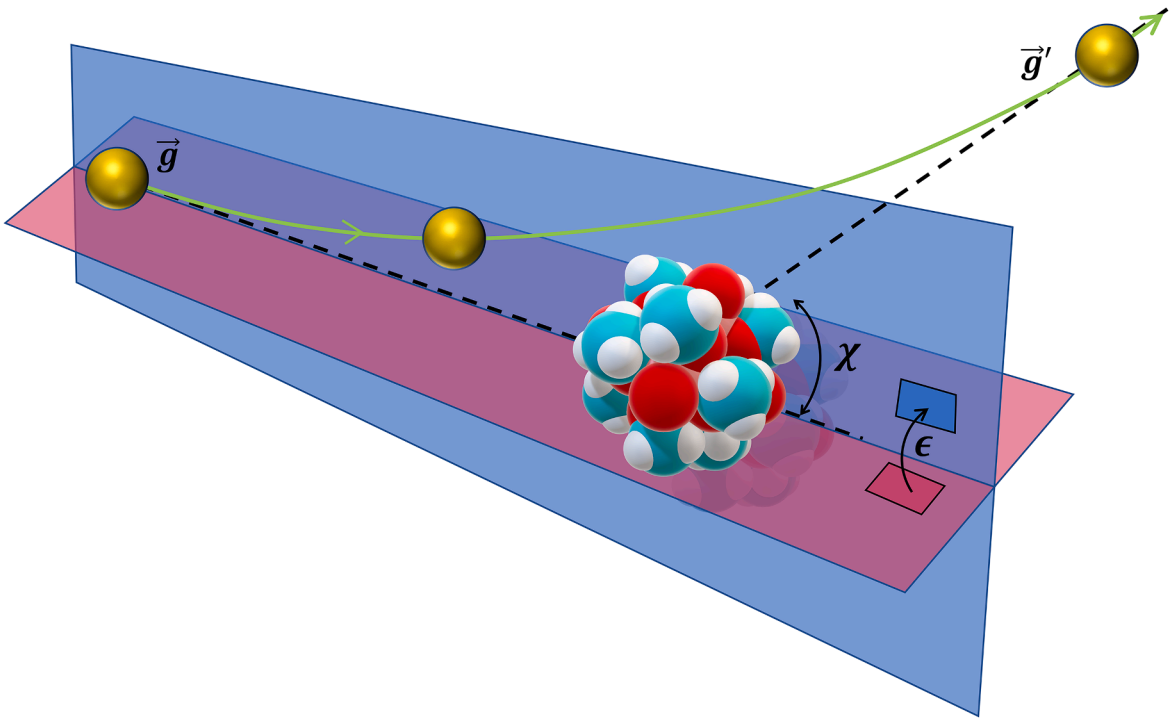

Fig. 1. Representation of a gas-ion trajectory in 3D. The gas molecule with the velocity $\vec{g}$ is being deflected by an angle χ. The trajectory plane (blue) makes an angle ϵ with respect to a fixed reference plane (red). (Adapted from Vincenti and Kruger [74], and Larriba and Prell [9]).

$$\left(\psi_{lm}^{(r)}, \psi_{pq}^{(s)}\right) = \frac{\Gamma\left(l+s+\frac{3}{2}\right)(l+|m|)!}{(2l+1)s!\Gamma\left(\frac{3}{2}\right)(l-|m|)!}\delta_{lp}\delta_{mq}\delta_{rs} \tag{7}$$

where, Γ and δ_{lp} indicates Gamma and Kronecker Delta functions respectively. One must now make an informed guess regarding what the general solution to the operator in Eq. (3) might be. Since it is expected for the gas-ion interaction to be close to the Maxwell model [33,34], the operator may be expanded using Burnett functions [35,36]:

$$\mathscr{J}\psi_{lm}^{(r)} = \sum_s a_{rs}(l)\psi_{lm}^{(s)} \tag{8}$$

where, the sum of s goes from 0 to infinity. The choice of Eq. (8) stems from the fact that for the Maxwell model and the one-temperature theory, $\mathscr{J}_{Maxwell}\psi_{lm}^{(r)} = \lambda_l^{(r)}\psi_{lm}^{(r)}$, where $\lambda_l^{(r)}$ and $\psi_{lm}^{(r)}$ are the eigenvalues and eigenvectors of the $\mathscr{J}_{Maxwell}$ operator. For other cases, one may assume that the $a_{rs}(l)$ are matrix elements that are larger the closer they are to the diagonal terms $a_{rr}(l)$ [37]. For the two-temperature theory using the Maxwell model, the off-diagonal terms are not zero, although they vanish for $s > r$ (more on this below). Using the orthogonal relation and Eq. (8), the matrix elements may be given by:

$$a_{rs}(l) = \frac{\left(\psi_{lm}^{(s)}, \mathscr{J}\psi_{lm}^{(r)}\right)}{\left(\psi_{lm}^{(s)}, \psi_{lm}^{(s)}\right)} \tag{9}$$

The matrix elements happen to be independent of the m index which can be dropped from the Burnett functions ($m = 0$) [35]. Making use of the recurrence relations of the Sonine and Legendre polynomials [10]:

$$\frac{d}{dx}S_p^{(n)}(x) = -S_{p+1}^{(n-1)}(x) \tag{10a}$$

$$\frac{x^2-1}{n}\frac{d}{dx}P_n(x) = xP_n(x) - P_{n-1}(x) \tag{10b}$$

$$pS_p^{(n)}(x) - xS_{p+1}^{(n-1)}(x) = (p+n)S_{p-1}^{(n)}(x) \tag{10c}$$

$$(2n+1)xP_n(x) - (n+1)P_{n+1}(x) = nP_{n-1}(x) \tag{10d}$$

as well as Eq. (8), Eq. (3) may be written as (dropping the subscript Av and the index m) [8]:

$$\left(l+\frac{1}{2}\right)\sum_s a_{rs}(l) < \psi_l^{(s)} >= \mathscr{E}\left[l\left(l+\frac{1}{2}+r\right) < \psi_{l-1}^{(r)} > - (l+1) < \psi_{l+1}^{(r-1)} >\right] \tag{11}$$

where, $\psi_l^{(s)} = 0$ for any negative index, $\psi_0^{(0)} = 1$, and where [38,39]:

$$\mathscr{E} = \left(\frac{eE}{Mn}\right)\left(\frac{M}{2kT_b}\right)^{\frac{1}{2}} \tag{12}$$

How to arrive at Eq. (11) from Eq. (3) and the recurrence relations Eqs. (10a-d) are shown in the supplementary information. In Eq. (11), only the matrix elements and the temperature T_b are unknown. Eq. (11) is an infinite set of coupled equations with an infinite sum. Given that direct averages of the Burnett functions cannot be obtained without explicitly knowing $F(z_i)$ (except for very particular cases [34,39–43]), an iterative form is sought. To avoid the infinite sum, the procedure is to add one additional term over those of the Maxwell model ($s > r = 0$) to the sum for every higher order approximation [10,25]. As such, the truncation scheme may look like:

$$\left(l+\frac{1}{2}\right)a_{rr}(l) < \psi_l^{(r)} >_n = \mathscr{E}\left[l\left(l+\frac{1}{2}+r\right) < \psi_{l-1}^{(r)} >_{n-1} - (l+1) < \psi_{l+1}^{(r-1)} >_{n-1}\right] - \left(l+\frac{1}{2}\right)\sum_{s=0}^{s=r-1} a_{rs}(l) < \psi_l^{(s)} >_n - \left(l+\frac{1}{2}\right)\sum_{s=r+1}^{s=n+r-1} a_{rs}(l) < \psi_l^{(s)} >_{n+r-s} \tag{13}$$

where, the subindex n stands for the order of approximation (not to be confused with the gas density). Note that the summation index is kept from $s = 0$ to $n + r - 1$, so that all terms up to $s = r$ always appear and

the upper summation terms are subsequently added for higher approximations. Mason has tried a different approximation type by using $n-1$ instead of n on the third term (first summation) on the right-hand side with similar success [11]. The last term of the right-hand side has an approximation $n+r-s$. The reason for this particular choice lies on the idea that each approximation contains only one additional $(E/n)^{2x}$ term in their sum [11]. Note also that the minimum order is 1 for the terms with approximation $n-1$ (there is no 0th approximation).

To obtain the ion's mobility, the Burnett function (from Eq. (5)) $< \psi_1^{(0)} > = \langle \left(\frac{M}{2kT_b}\right)^{1/2} w \rangle = \left(\frac{M}{2kT_b}\right)^{1/2} v_d$ may be used and where $v_d = KE$ is the average drift velocity of the ion, being K the mobility. Using this equation and Eq. (13), the first approximation may be given by:

$$a_{00}(1) < \psi_1^{(0)} >_I = \mathscr{E} \text{ or } K_I = \frac{\left(\frac{e}{Mn}\right)}{a_{00}(1)} \tag{14}$$

where, $a_{00}(1)$ would need to be calculated but it is dependent on the base temperature whose value needs to be provided. Advancing the value of the matrix element (to be calculated below), the typical Mason-Schamp expression appears [16,26]:

$$K_I = \frac{3e}{16n}\sqrt{\frac{2\pi}{\mu k T_{eff}}}\frac{1}{\Omega^{(1,1)}(T_{eff})} \tag{15}$$

where, μ is the reduced mass and $\Omega^{(1,1)}(T_{eff})$ is the momentum transfer collision integral calculated at the effective temperature T_{eff} which may be related to T_b through [9,44]:

$$T_{eff} = \frac{MT + mT_b}{M+m} \tag{16}$$

The physical importance of T_{eff} will be described below. Before continuing to higher-order approximations, it is important to establish a relationship between the base temperature T_b (or T_{eff}) and the field over concentration E/n. T_b, as advanced previously, can be chosen to be the ion's temperature in the laboratory frame, but any other choice could have been equally valid (and perhaps more optimal for convergence) [22,39,45–47]. With this choice, T_b is given by:

$$\frac{1}{2}M < z^2 > = \frac{3}{2}kT_b \tag{17}$$

Eq. (17) is equivalent to $< \psi_0^{(1)} > = 0$. Using Eq. (13) with $< \psi_0^{(1)} >$ will allow us to find an equation that establishes the relation between E/n (or $\mathscr{E}$) and T_b.

2.1. Higher order approximations

By repeated application of Eq. (13) one can reach higher-order approximations that may be generally written as [48]:

$$< K >_n = < K >_I \left[\alpha_0 + \alpha_1\left(\frac{\mathscr{E}}{a_{00}(1)}\right)^2 + \alpha_2\left(\frac{\mathscr{E}}{a_{00}(1)}\right)^4 + \ldots + \alpha_{n-1}\left(\frac{\mathscr{E}}{a_{00}(1)}\right)^{2(n-1)}\right] \tag{18}$$

where, the number of higher-order terms depends on the approximation n. Here, the α_i coefficients are complicated functions of the matrix elements. For example, the second approximation may be given by (Eq. (13)):

$$< \psi_1^{(0)} >_{II} = \frac{\mathscr{E}}{a_{00}(1)} - \frac{a_{01}(1)}{a_{00}(1)} < \psi_1^{(1)} >_I \tag{19}$$

Note the second term on the right-hand side (neglected in the first approximation) appears from the summation term since it is now terminated at $s = 2+0-1 = 1$. The first approximation for the Burnett function of the second term is given by:

$$< \psi_1^{(1)} >_I = \frac{\mathscr{E}}{a_{11}(1)}\left[\frac{5}{3} < \psi_0^{(1)} >_I - \frac{4}{3} < \psi_2^{(0)} >_I\right] - \frac{a_{10}(1)}{a_{11}(1)} < \psi_1^{(0)} >_I \tag{20}$$

In Eq. (20), the additional last term on the right-hand side comes in this case from the summation when $s = 0$. The functions in the brackets may now be given by:

$$< \psi_0^{(1)} >_I = -\frac{2\mathscr{E}}{a_{11}(0)} < \psi_1^{(0)} >_I - \frac{a_{10}(0)}{a_{11}(0)} \tag{21}$$

$$< \psi_2^{(0)} >_I = \frac{2\mathscr{E}}{a_{00}(2)} < \psi_1^{(0)} >_I \tag{22}$$

The second term in Eq. (21) comes from assuming the Maxwell condition for the first approximation where terms $s \le r$ are added. However, having established Eq. (17) ($< \psi_0^{(1)} > = 0$), then Eq. (21) is no longer needed. Putting all the terms together and simplifying, we arrive at the second approximation to the two-temperature theory:

$$< \psi_1^{(0)} >_{II} = < \psi_1^{(0)} >_I \left[1 + \frac{a_{01}(1)a_{10}(1)}{a_{00}(1)a_{11}(1)} + \frac{5}{3}\frac{a_{01}(1)a_{10}(0)}{a_{11}(0)a_{11}(1)} + \left(\frac{\mathscr{E}}{a_{00}(1)}\right)^2\left(\frac{8}{3}\frac{a_{01}(1)a_{00}(1)}{a_{00}(2)a_{11}(1)} + \frac{10}{3}\frac{a_{01}(1)a_{00}(1)}{a_{11}(0)a_{11}(1)}\right)\right] \tag{23}$$

or:

$$< \psi_1^{(0)} >_{II} = < \psi_1^{(0)} >_I \left[1 + \frac{a_{01}(1)a_{10}(1)}{a_{00}(1)a_{11}(1)} + \left(\frac{\mathscr{E}}{a_{00}(1)}\right)^2\left(\frac{8}{3}\frac{a_{01}(1)a_{00}(1)}{a_{00}(2)a_{11}(1)}\right)\right] \tag{24}$$

when Eq. (17) is considered. Eq. (19) now becomes an equation to establish the relationship between E/n and T_b. Note how aside from the quadratic term that depends on the field $\left(\frac{\mathscr{E}}{a_{00}(1)}\right)^2$, an additional term appears to correct the expression for mobility even at the zero field.

For the third approximation, we proceed in a similar way. The main equation may be given by:

$$< \psi_1^{(0)} >_{III} = \frac{\mathscr{E}}{a_{00}(1)} - \frac{a_{01}(1)}{a_{00}(1)} < \psi_1^{(1)} >_{II} - \frac{a_{02}(1)}{a_{00}(1)} < \psi_1^{(2)} >_I \tag{25}$$

where, the third term appears due to the fact that the summation now terminates at $s = 3+0-1 = 2$. The functions on the right-hand side may also include additional terms as well due to their higher order. As such:

$$< \psi_1^{(1)} >_{II} = \frac{\mathscr{E}}{a_{11}(1)}\left[\frac{5}{3} < \psi_0^{(1)} >_I - \frac{4}{3} < \psi_2^{(0)} >_I\right] - \frac{a_{10}(1)}{a_{11}(1)} < \psi_1^{(0)} >_I - \frac{a_{12}(1)}{a_{11}(1)} < \psi_1^{(2)} >_I = < \psi_1^{(1)} >_I - \frac{a_{12}(1)}{a_{11}(1)} < \psi_1^{(2)} >_I \tag{26}$$

$$< \psi_1^{(2)} >_I = \frac{\mathscr{E}}{a_{22}(1)}\left[\frac{7}{3}< \psi_0^{(2)} >_I - \frac{4}{3}< \psi_2^{(1)} >_I\right] - \frac{a_{20}(1)}{a_{22}(1)}< \psi_1^{(0)} >_I - \frac{a_{21}(1)}{a_{22}(1)}< \psi_1^{(1)} >_I \tag{27}$$

$$< \psi_0^{(2)} >_I = -\frac{2\mathscr{E}}{a_{22}(0)}< \psi_1^{(1)} >_I - \frac{a_{20}(0)}{a_{22}(0)} - \frac{a_{21}(0)}{a_{22}(0)}< \psi_0^{(1)} >_I \tag{28}$$

$$< \psi_2^{(1)} >_I = \frac{\mathscr{E}}{a_{11}(2)}\left[\frac{14}{5}< \psi_1^{(1)} >_I - \frac{6}{5}< \psi_3^{(0)} >_I\right] - \frac{a_{10}(2)}{a_{11}(2)}< \psi_2^{(0)} >_I \tag{29}$$

$$< \psi_3^{(0)} >_I = \frac{3\mathscr{E}}{a_{00}(3)}< \psi_2^{(0)} >_I \tag{30}$$

Note that $< \psi_1^{(2)} >_I$ is only a first approximation instead of a second. This is due to the choice of reducing the approximation of the extra terms to $n+r-s$. If the second approximation were used instead in Eq. (25), it would bring higher powers of E/n. There is no necessity to substitute the different functions Eqs. (26)–((30)) to provide a full expression for the third approximation as it becomes unmanageable. The fourth approximation may equally be written to be:

$$< \psi_1^{(0)} >_{IV} = \frac{\mathscr{E}}{a_{00}(1)} - \frac{a_{01}(1)}{a_{00}(1)}< \psi_1^{(1)} >_{III} - \frac{a_{02}(1)}{a_{00}(1)}< \psi_1^{(2)} >_{II} - \frac{a_{03}(1)}{a_{00}(1)}< \psi_1^{(3)} >_I \tag{31}$$

Higher-order expressions can be easily obtained but are omitted here as they start to become too large to handle analytically.

2.2. Ion's energy

One of the most difficult endeavors when dealing with the two-temperature approximation is establishing the relation between the field over the concentration E/n and the temperature T_b (or similarly T_{eff}) [19,39,49–53]. The reason for this is that the temperature T_b is a parameter used in the base function to describe that the ion's velocity distribution is skewed (displaced) by the drift velocity v_d and its standard deviation is larger due to field-related heating over the thermal equilibrium with the gas [39,54]. Choosing $T_b = T_{ion}$ (temperature of the ion in the laboratory frame) establishes some important considerations. The first one is that $\frac{3}{2}kT_b = \frac{1}{2}m < z^2 >$ so that the ion's energy can be directly related to T_b. One would expect therefore that calculating the ion's energy moment $< \psi_0^{(1)} >$ would be sufficient. As advanced previously the moment yields: $< \psi_0^{(1)} > = \frac{3}{2} - \frac{M<z^2>}{2kT_b} = 0$. However, Eq. (13) may still be used to provide a relation between ion temperature and field. The degree of accuracy used to establish a relation between T_b and E/n can be any, but it is preferred to match the order of approximation of mobility. For example, for the first approximation:

$$\frac{1}{2}a_{11}(0)< \psi_0^{(1)} >_I = 0 = -\mathscr{E}< \psi_1^{(0)} >_I - \frac{1}{2}a_{10}(0)< \psi_0^{(0)} >_I \tag{32}$$

Or:

$$\mathscr{E} = -\frac{1}{2}\frac{a_{10}(0)}{< \psi_1^{(0)} >_I} \rightarrow \mathscr{E}^2 = -\frac{1}{2}\, a_{10}(0)a_{00}(1) \tag{33}$$

To physically understand the meaning of Eq. (33), the expressions of the matrix elements (see their calculation below) must be introduced to yield a first approximation for E/n:

$$\left(\frac{E}{n}\right)^2 = \frac{128}{3}\frac{\mu}{M+m}\frac{k^2T_{eff}}{e^2}\left(\frac{T_b - T}{\pi}\right)\Omega^{(1,1)^2}(T_{eff}) \tag{34}$$

This result coincides with Wannier's equation [1,39]:

$$\frac{3}{2}kT_b = \frac{3}{2}kT + \frac{1}{2}(m+M)< w >^2 = \frac{3}{2}kT + \frac{1}{2}(m+M)< K >_I^2 E^2 \tag{35}$$

This can be proven by using the solution from the first approximation to mobility $< K >_I = \frac{e}{Mn}\frac{1}{a_{00}(1)}$ in Eq. (35) arriving at Eq. (34). For the first approximation, it can also be shown from the relation between T_b and T_{eff} that $\frac{3}{2}kT_{eff} = \frac{3}{2}kT + \frac{1}{2}m< w >^2$ which has important consequences [23,55,56]. Eq. (35), while it is only a first-order approximation to the ion's energy, it does provide a simple physical explanation of the two characteristic temperatures. $\frac{1}{2}M< w >^2$ corresponds to the total field energy required for the ion to go from thermal equilibrium to its drift velocity [57–59] given it is the ion's kinetic energy. This value is quite large so T_b can easily be in the tens of thousands of Kelvins, and it is not a good measure of the ion's thermodynamic temperature [45,60–63]. However, subtracting the ion's kinetic energy $\frac{1}{2}M< w >^2$, the rest can be regarded as its translational thermal molecular energy which corresponds to $\frac{3}{2}kT_{eff}$ and where $\frac{1}{2}m< w >^2$, corresponds to the thermal translational energy increase due to the higher relative velocity collisions with the gas. In this sense, the effective temperature is the ion's equilibrium temperature due to the combination of the gas temperature and the effect of the field (assuming elastic collisions) [64–67].

For the second approximation, Viehland assumes that $\mathscr{E}$ can be thought of as having approximations in a similar way to the Burnett functions, e.g., $\mathscr{E}_n$. Viehland uses Eq. (13) for $< \psi_1^{(0)} >$ as well as $< \psi_0^{(1)} > = 0$ and combines them to arrive at [24]:

$$\frac{2\mathscr{E}_n}{a_{00}(1)} = \sum_{s=1}^{n-1}\frac{a_{0s}(1)}{a_{00}(1)}< \psi_1^{(s)} >_{n-s} + \left\{\begin{array}{l}\left[\sum_{s=1}^{n-1}\frac{a_{0s}(1)}{a_{00}(1)}< \psi_1^{(s)} >_{n-s}\right]^2 - \\ 2\left[\frac{a_{10}(0)}{a_{00}(1)} + \sum_{s=2}^{n}\frac{a_{0s}(1)}{a_{00}(1)}< \psi_0^{(s)} >_{n+1-s}\right]\end{array}\right\}^{\frac{1}{2}} \tag{36}$$

A different approach to obtain higher approximations of the ion's energy is to use the recursive Eq. (13) relation for $< \psi_0^{(1)} >$ but assuming that $\mathscr{E}$ is a constant to be calculated. This leads to a polynomial equation of powers of $\mathscr{E}^2$. For example, for the second approximation:

$$\frac{1}{2}a_{11}(0)< \psi_0^{(1)} >_{II} = 0 = -\mathscr{E}< \psi_1^{(0)} >_I - \frac{1}{2}a_{10}(0) - \frac{1}{2}a_{12}(0)< \psi_0^{(2)} >_I \tag{37}$$

$$\mathscr{E}_{II}^2 = -\frac{1}{2}\, a_{10}(0)a_{00}(1) - \frac{\mathbf{1}}{\mathbf{2}}\boldsymbol{a_{00}(1)a_{12}(0)}< \boldsymbol{\psi_0^{(2)}} >_I \tag{38}$$

Substituting the appropriate approximations leads to a quadratic equation for $\mathscr{E}^2$:

$$A\mathscr{E}_{II}^4 + B\mathscr{E}_{II}^2 + C = 0 \tag{39}$$

With:

$$A = \frac{8}{3}\frac{a_{12}(0)}{a_{11}(1)a_{00}(2)a_{22}(0)}$$

$$B = 1 + \frac{a_{10}(1)a_{12}(0)}{a_{11}(1)a_{22}(0)}$$

$$C = \frac{1}{2}a_{00}(1)\left(a_{10}(0) - \frac{a_{20}(0)a_{12}(0)}{a_{22}(0)}\right)$$

The solution that is chosen for the quadratic equation is the closest to that of the first approximation as it is expected that in Eq. (38) the bold term is a small correction. Using the same process, higher-order terms may be obtained. For the third:

$$\mathscr{E}< \psi_1^{(0)} >_{III} = -\frac{1}{2}\, a_{10}(0) - \frac{\mathbf{1}}{\mathbf{2}}\boldsymbol{a_{12}(0)}< \boldsymbol{\psi_0^{(2)}} >_{II} - \frac{\mathbf{1}}{\mathbf{2}}\boldsymbol{a_{13}(0)}< \boldsymbol{\psi_0^{(3)}} >_I \tag{40}$$

And where the full expanded equation for $\mathscr{E}_{III}$ has been added to the

supplementary information. Whether this method or an iterative method is employed, the relation between T_b and E/n should be established and it is expected to have only a scaling effect over the values of mobility as a function of the field.

It is important to note that, regardless of which method is employed, once $\mathscr{E}$ is calculated for a particular order of approximation, its value is fixed in the expression for mobility as different values of $\mathscr{E}$ would lead to different $T_b - E/n$ relations.

3. Calculation of the matrix elements

At this point, the matrix elements need to be calculated to obtain detailed expressions for mobility as a function of the field. However, the matrix elements can only be analytically calculated for extremely simple potentials (like that of Maxwell) assuming monoatomic ions. For the rest of the cases, the matrix elements' expressions can be left as a quadrature that may be integrated numerically by calculating the deflection angle [68–71]. Aisbett produced a general formula to obtain all the different matrix elements (see supplementary information or refer to Ref. [26]). The formula provided by Viehland contains a small error (a factor of 2 corrected here) that will not affect the mobility results [11]. It is however unadvisable to use the formula without prior knowledge of how the matrix coefficients are calculated. This exercise also serves the purpose that it can be used with any other orthogonal functions for which general formulas do not exist. The procedure of how the calculation is performed is laid out initially, followed by explicit solutions of some of the terms. The rest of the terms needed up to the third approximation have been added to the supplementary information, where many of them are also explicitly calculated.

Each matrix element must be obtained using Eq. (9). While the denominator is given by Eq. (7) (assuming $m = 0$), the numerator is given by Larriba-Andaluz and Prell [9]:

$$\left(\psi_l^{(s)}, \mathscr{J}\psi_l^{(r)}\right) = \left(\frac{M}{2\pi kT_b}\right)^{\frac{3}{2}}\left(\frac{m}{2\pi kT}\right)^{\frac{3}{2}}\int\int\int\int e^{\left(-\frac{Mc^2}{2kT_b}\right)} e^{\left(-\frac{mc^2}{2kT}\right)} \times\psi_l^{(s)}(\vec{z})\left[\psi_l^{(r)}(\vec{z}) - \psi_l^{(r)}(\vec{z}')\right]|\vec{z} - \vec{c}|bdbd\epsilon d\vec{z}d\vec{c} \tag{41}$$

Here, we have opted to use the more conventional vector notation instead of an index notation. The differential $d\vec{z} = dz_1dz_2dz_3$ stands for a triple integral over the three velocity directions and $\times$ stands for a regular multiplication to indicate a change of line. It is assumed that the gas has a fixed Maxwell–Boltzmann velocity distribution (f) at temperature T [72,73]. To make Eq. (41) more accessible, assuming a two-body problem, the independent velocity variables are changed into the relative velocity $\vec{g}$ and the centre of mass velocity $\vec{W}$:

$$\vec{z} - \vec{c} = \vec{g}$$

$$\vec{W} = (1 - e_\mu)\vec{z} + e_\mu\vec{c};\ e_\mu = \frac{m}{m+M}$$

so that the matrix elements become:

$$a_{rs}(l) = \frac{(2l+1)s!\Gamma\left(\frac{3}{2}\right)}{\Gamma\left(l+s+\frac{3}{2}\right)}\left(\frac{M}{2\pi kT_b}\right)^{\frac{3}{2}}\left(\frac{m}{2\pi kT}\right)^{\frac{3}{2}} \times\int\int\int\int e^{\left(-\left(\frac{M}{2kT_b}+\frac{m}{2kT}\right)W^2+2\mu\left(\frac{1}{2kTb}-\frac{1}{2kT}\right)\vec{W}\cdot\vec{g}+\frac{\mu}{m+M}\left(\frac{m}{2kT_b}+\frac{M}{2kT}\right)g^2\right)} \times\psi_l^{(s)}\left(\vec{W}+e_\mu\vec{g}\right)\left[\psi_l^{(r)}\left(\vec{W}+e_\mu\vec{g}\right) - \psi_l^{(r)}\left(\vec{W}+e_\mu\vec{g}'\right)\right]gbdbd\epsilon d\vec{W}d\vec{g} \tag{42}$$

Where the interpretation of the prime remains the same. Given the complexity of the exponential in Eq. (42), it is advisable to make a change of variables that will make it quadratic:

$$\vec{W}_q = \vec{W} - f\vec{g};\ d\vec{W}d\vec{g} = d\vec{W}_q d\vec{g}$$

where,

$$f = e_\mu d\frac{M(T_b - T)}{mT_b};\ d = \frac{mT_b}{MT + mT_b};\ e_\mu + f = d;\ e_\mu M = \mu$$

Dropping the q in W_q (for extra cleanliness) one arrives at:

$$a_{rs}(l) = \frac{(2l+1)s!\Gamma\left(\frac{3}{2}\right)}{\Gamma\left(l+s+\frac{3}{2}\right)}\left(\frac{M}{2\pi kT_b}\right)^{\frac{3}{2}}\left(\frac{m}{2\pi kT}\right)^{\frac{3}{2}} \times\int\int\int\int e^{\left(-\left(\frac{m}{2kT}\right)W^2-\left(\frac{\mu}{2kT_{eff}}\right)g^2\right)} \times\psi_l^{(s)}\left(\vec{W}+d\vec{g}\right)\left[\psi_l^{(r)}\left(\vec{W}+e_\mu\vec{g}+f\vec{g}\right) - \psi_l^{(r)}\left(\vec{W}+e_\mu\vec{g}'+f\vec{g}\right)\right]gbdbd\epsilon d\vec{W}d\vec{g} \tag{43}$$

Eq. (43) may be used as the basis for the matrix element calculations. After simplifications, the matrix elements may be expressed using conventional collision integrals which are given by McDaniel and Mason [13,18]:

$$\Omega^{(l,s)}(T) = \frac{2}{(s+1)!}\left(\frac{\mu}{2kT}\right)^{s+2}\int_0^\infty e^{-\left(\frac{\mu}{2kT}\right)g^2} g^{2s+3}Q^{(l)}(g)dg \tag{44}$$

$$Q^{(l)} = 2\pi\left(\frac{2(l+1)}{2l+1-(-1)^l}\right)\int_0^\infty\left(1 - \cos^l\chi(b)\right)bdb \tag{45}$$

The coefficients in Eqs. (44) and (45) are traditionally added so that the value of both integrals is πd^2 for a hard sphere of diameter of influence (radius of gas plus ion) d. The calculation of the matrix elements is now tedious but straightforward. To start, several examples are shown which are relevant to important discussions, while the rest of the calculations will be added to the supplementary information which includes further elements never previously calculated.

3.1. Calculation of $a_{00}(1)$

Given that $\psi_1^{(0)} = w\left(\frac{M}{2kT_b}\right)^{1/2} = z_1\left(\frac{M}{2kT_b}\right)^{1/2}$ with $\vec{z} = (z_1 = w, z_2, z_3)$ and the following expressions:

$$\frac{(2l+1)s!\Gamma\left(\frac{3}{2}\right)}{\Gamma\left(l+s+\frac{3}{2}\right)}|_{l=1,s=0} = 2,$$

$$\psi_l^{(0)}\left(\vec{W}+d\vec{g}\right)\left[\psi_l^{(0)}\left(\vec{W}+e_\mu\vec{g}+f\vec{g}\right) - \psi_l^{(0)}\left(\vec{W}+e_\mu\vec{g}'+f\vec{g}\right)\right] = \frac{e_\mu M(g_1 - g_1')(dg_1 + W_1)}{2kT_b},$$

one arrives at the integral to solve the matrix element:

$$a_{00}(1) = 2\left(\frac{M}{2\pi kT_b}\right)^{\frac{3}{2}}\left(\frac{m}{2\pi kT}\right)^{\frac{3}{2}} \times\int\int\int\int e^{\left(-\left(\frac{m}{2kT}\right)W^2-\left(\frac{\mu}{2kT_{eff}}\right)g^2\right)}\frac{e_\mu M(g_1 - g_1')(dg_1 + W_1)}{2kT_b}gbdbd\epsilon d\vec{W}d\vec{g} \tag{46}$$

One can now integrate the center of mass velocity W from $-\infty$ to ∞ for all three coordinates. This yields:

$$a_{00}(1) = 2\left(\frac{M}{2\pi kT_b}\right)^{\frac{3}{2}}\left(\frac{m}{2\pi kT}\right)^{\frac{3}{2}} \times \int\int\int e^{\left(-\left(\frac{\mu}{2kT_{eff}}\right)g^2\right)}\frac{\sqrt{2}de_\mu M}{kT_b}\left(\frac{\pi dkT}{m}\right)^{\frac{3}{2}}(g_1 - g_1^{'})g_1 g b d b d\epsilon d\vec{g} \quad (47)$$

To continue the integration, it is necessary to define proper general vectors for $\vec{g}$ and $\vec{g}^{'}$. Using cartesian coordinates and spherical angles, the relative velocity vector may be given by: $\vec{g} = (g_1, g_2, g_3) = g(\cos\theta_g, \sin\theta_g\cos\phi_g, \sin\theta_g\sin\phi_g)$, where θ_g and ϕ_g are the azimuthal and polar angle respectively. Due to the symmetry of elastic collisions and conservation of energy, $\vec{g}^{'}$ can be interpreted at this point as the relative velocity of reemission of the trajectory of a gas molecule with the ion fixed in a centered position as shown in Fig. 1. If the gas molecule trajectory direction was inverted, the result would be a replenishment of class $\vec{g}$ velocities from class $\vec{g}^{'}$. Fig. 1 can also be used to understand the deflection angle χ and the out-of-plane angle ϵ that can be used for the definition of $\vec{g}^{'}$:

$$\vec{g}^{'} = g(\cos\chi\ \hat{g} + \sin\chi\ \cos\epsilon\ \hat{e}_2 + \sin\chi\ \sin\epsilon\ \hat{e}_3) \quad (48)$$

where, $\hat{g}$ is a unit vector in the direction of $\vec{g}$ and $\hat{e}_2$ *and* $\hat{e}_3$ are unit vectors perpendicular to $\hat{g}$ and to each other. Note that due to the conservation of energy in the collision $\vec{g}$ and $\vec{g}^{'}$ have the same magnitude. In Cartesian coordinates, the second and third terms in Eq. (48) may be given by:

$$\vec{e}_{2_\perp} = g\left(0, -\sin(\phi_g), \cos(\phi_g)\right)\cos\epsilon\ \sin\chi \quad (49)$$

$$\vec{e}_{3_\perp} = g\left(\sin(\theta_g), -\cos(\phi_g)\cos(\theta_g), -\cos(\theta_g)\sin(\phi_g)\right)\sin\chi\ \sin\epsilon \quad (50)$$

which are much simpler and more efficient to use than those produced by Vincenti and Kruger [74]. Substituting the incident and reemitted relative velocity vectors and integrating Eq. (47) for ϵ between 0 and 2π yields:

$$\psi_1^{(2)}\left(\vec{W} + d\vec{g}\right)\left[\psi_1^{(0)}\left(\vec{W} + e_\mu\vec{g} + f\vec{g}\right) - \psi_1^{(0)}\left(\vec{W} + e_\mu\vec{g}^{'} + f\vec{g}\right)\right] = e_\mu M(g_1 - g_1^{'})(dg_1 + W_1)\left(\begin{array}{c} d^4M^2g^2 + 35k^2T_b^2 + 4d^3M^2g^2\vec{g}\cdot\vec{W} - 14kMT_bW^2 + \\ M^2W^4 + 4dM\vec{g}\cdot\vec{W}(MW^2 - 7kT_b) + 2d^2M\left(Mg^2W^2 - 7g^2kT_b + 2M\left(\vec{g}\cdot\vec{W}\right)\left(\vec{g}\cdot\vec{W}\right)\right) \end{array}\right) \Big/ 16k^3T_b^3$$

$$a_{00}(1) = 2\left(\frac{M}{2\pi kT_b}\right)^{\frac{3}{2}}d^{5/2}e_\mu\frac{M}{2kT_b}\int\int 2\pi(1-\cos\chi)bdb\ \ e^{\left(-\left(\frac{\mu}{2kT_{eff}}\right)g^2\right)}g_1^2 g d\vec{g}$$

Using the relation that $\frac{Md}{kT_b} = \frac{\mu}{kT_{eff}}$ and $dg_1dg_2dg_3 = g^2\sin\theta_g d\phi_g d\theta_g dg$:

$$a_{00}(1) = \frac{2}{\pi^{3/2}}\left(\frac{\mu}{2kT_{eff}}\right)^{\frac{5}{2}}\int_0^\infty\left[\int_0^\infty 2\pi(1-\cos\chi)bdb\right]\int_0^\pi\int_0^{2\pi}e^{\left(-\left(\frac{\mu}{2kT_{eff}}\right)g^2\right)}g^5\cos^2\theta_g\sin\theta_g d\phi_g d\theta_g dg$$

where the term in brackets is $Q^{(1)}(g)$. Integrating over the velocity angles and multiplying and dividing by $\left(\frac{\mu}{2kT_{eff}}\right)^{1/2}$:

$$a_{00}(1) = \frac{8}{3}e_\mu\left(\frac{2kT_{eff}}{\pi\mu}\right)^{\frac{1}{2}}\left[\left(\frac{\mu}{2kT_{eff}}\right)^3\int_0^\infty e^{\left(-\left(\frac{\mu}{2kT_{eff}}\right)g^2\right)}g^5Q^{(1)}(g)dg\right] \quad (51)$$

The term in brackets corresponds to $\Omega^{(1,1)}(T_{eff})$ so that:

$$a_{00}(1) = \frac{8}{3}e_\mu\sqrt{\frac{2kT_{eff}}{\pi\mu}}\,\Omega^{(1,1)}(T_{eff}) \quad (52)$$

A dimensionless matrix coefficient can be obtained by dividing Eq. (52) by $e_\mu\sqrt{\frac{2kT_{eff}}{\pi\mu}}\,\Omega^{(1,1)}(T_{eff})$:

$$a_{00}^*(1) = \frac{a_{00}(1)}{e_\mu\sqrt{\frac{2kT_{eff}}{\pi\mu}}\,\Omega^{(1,1)}(T_{eff})} = \frac{8}{3} \quad (53)$$

This coefficient is fundamental in obtaining the first approximation to mobility as shown in Eq. (14).

3.2. Calculation of $a_{02}(1)$

Given the following identities:

$$\psi_1^{(0)} = w\left(\frac{M}{2kT_b}\right)^{\frac{1}{2}},\ \psi_1^{(2)} = \frac{1}{2}w\left(\frac{M}{2kT_b}\right)^{\frac{1}{2}}\left[\frac{35}{4} - 7\frac{M}{2kT_b}z^2 + \left(\frac{M}{2kT_b}\right)^2z^4\right],$$

$$\vec{z} = (z_1 = w, z_2, z_3).$$

$$\frac{(2l+1)s!\Gamma\left(\frac{3}{2}\right)}{\Gamma\left(l+s+\frac{3}{2}\right)}\Big|_{l=1,s=2} = \frac{16}{35}$$

Substituting the above into Eq. (43) and integrating over the center of mass velocities and over the polar angle ϵ yields:

$$a_{02}(1) = \frac{4}{35\pi^{\frac{1}{2}}}e_\mu\left(\frac{\mu}{2kT_{eff}}\right)^{\frac{5}{2}}\int\int e^{\left(-\left(\frac{\mu}{2kT_{eff}}\right)g^2\right)}\frac{1}{m^2k^2T_b^2}\left[d^2M^2\left(d^2g^2m^2 + 14dg^2kmT + 35k^2T^2\right) - 14dkmMT_b\left(dg^2m + 5kT\right) + 35m^2k^2T_b^2\right]g_1^2(1-\cos(\chi))g2\pi bdbd\vec{g}$$

Integrating over the velocity angles and arranging:

$$a_{02}(1) = \frac{8}{105\pi^{\frac{1}{2}}} e_\mu \left(\frac{\mu}{2kT_{eff}}\right)^{\frac{5}{2}} \int\int e^{\left(-\left(\frac{\mu}{2kT_{eff}}\right)g^2\right)} \times \left[d^2 g^4 \left(\frac{dM}{kT_b}\right)^2 + 14dg^2 \left(\frac{dM}{kT_b}\right)\left(\frac{MTd}{mT_b}\right) + 35\left(\frac{MTd}{mT_b}\right)^2 - 14\left(dg^2\left(\frac{dM}{kT_b}\right) + 5\left(\frac{MTd}{mT_b}\right)\right) + 35\right] g^5 (1-\cos(\chi)) 2\pi bdbdg$$

Using the CCS relations and the identities $\frac{Md}{kT_b} = \frac{\mu}{kT_{eff}}$ and $\frac{dMT}{mT_b} = (1-d)$ one can write:

$$a_{02}(1) = \frac{8}{105} e_\mu \left(\frac{2kT_{eff}}{\mu\pi}\right)^{\frac{1}{2}} \Omega^{(1,1)} \left[48d^2 \frac{\Omega^{(1,3)}}{\Omega^{(1,1)}} + 84d(1-d)\frac{\Omega^{(1,2)}}{\Omega^{(1,1)}} + 35(1-d)^2 - 84d\frac{\Omega^{(1,2)}}{\Omega^{(1,1)}} - 70(1-d) + 35\right]$$

Simplifying, rearranging, and using the common relations $C^* = \frac{\Omega^{(1,2)}(T_{eff})}{\Omega^{(1,1)}(T_{eff})}$ and $B^* = 5C^* - 4\frac{\Omega^{(1,3)}(T_{eff})}{\Omega^{(1,1)}(T_{eff})}$:

$$a_{02}(1) = -\frac{8d^2}{105} e_\mu \left(\frac{2kT_{eff}}{\mu\pi}\right)^{\frac{1}{2}} \Omega^{(1,1)} [3(4B^* - 5) + 4(6C^* - 5)]$$

Hence:

$$a_{02}^*(1) = -\frac{8d^2}{105}[3(4B^* - 5) + 4(6C^* - 5)] \quad (54)$$

The expressions are written following the behavior of the Maxwell model and the reason for such choice will be clarified in the discussion below.

3.3. Calculation of $a_{21}(0)$

Given that $\psi_0^{(1)} = \frac{3}{2} - z^2\left(\frac{M}{2kT_b}\right)$, $\psi_0^{(2)} = \frac{1}{2}\left(\frac{15}{4} + \frac{M^2 g^4}{4k^2T_b^2} - \frac{5Mz^2}{2kT_b}\right)$, $\vec{z} = (z_1 = w, z_2, z_3)$

$$\frac{(2l+1)s!\,\Gamma\left(\frac{3}{2}\right)}{\Gamma\left(l+s+\frac{3}{2}\right)}\Big|_{l=0,s=1} = \frac{2}{3}$$

$$\psi_0^{(1)}\left(\vec{W} + d\vec{g}\right)\left[\psi_0^{(2)}\left(\vec{W} + e_\mu\vec{g} + f\vec{g}\right) - \psi_0^{(2)}\left(\vec{W} + e_\mu\vec{g}' + f\vec{g}\right)\right] = -\frac{e_\mu M\left(f(g^2 - \vec{g}\cdot\vec{g}') + \vec{W}\cdot(\vec{g} - \vec{g}')\right)\left(M\left(d^2g^2 + W^2 + 2d\left(\vec{g}\cdot\vec{W}\right)\right)\right)}{8k^3T_b^3}$$
$$\left(M\left(2e_\mu g^2 + 2e_\mu\left(f\left(g^2 + \vec{g}\cdot\vec{g}'\right) + \vec{W}\cdot(\vec{g} + \vec{g}')\right)\right) + 2\left(f^2g^2 + W^2 + 2f\vec{g}\cdot\vec{W}\right)\right) - 10kT_b\right)$$

Integrating over the center of mass velocities, over epsilon, and over the velocity angles yields:

$$a_{21}(0) = -\frac{4}{3d\pi^{\frac{1}{2}}} e_\mu \left(\frac{\mu}{2kT_{eff}}\right)^{\frac{5}{2}} \int\int e^{\left(-\left(\frac{\mu}{2kT_{eff}}\right)g^2\right)} \frac{1}{m^2k^2T_b^2} \times \left[5d^3kM^2T\left(fg^2m + 2kT\right) + 3dfkmMT\left(\left(e_\mu^2 + f^2\right)g^2M - 10kT_b\right) - 3fkm^2T_b\left(\left(e_\mu^2 + f^2\right)g^2M - 5kT_b\right) + d^2M\left(M\left(f\left(e^2 + f^2\right)g^4m^2 + 2\left(e^2 + 3f^2\right)g^2kmT + 25fk^2T^2\right) - 5kmT_b\left(fg^2m + 2kT\right)\right) + e_\mu fg^2mM\left(dM\left(dfg^2m + 4dkT + 3fkT\right) - 3fkmT_b\right)(1 + \cos(\chi))\right] g^5(1 - \cos(\chi))2\pi bdbdg$$

Rearranging:

$$a_{21}(0) = -\frac{4}{3d\pi^{\frac{1}{2}}} e_\mu \left(\frac{\mu}{2kT_{eff}}\right)^{\frac{5}{2}} \int\int e^{\left(-\left(\frac{\mu}{2kT_{eff}}\right)g^2\right)} \left[5\left(\frac{dM}{kT_b}\right)\left(\frac{MTd}{mT_b}\right)fdg^2 + 10\left(\frac{MTd}{mT_b}\right)^2 d + 3\left(\frac{dM}{kT_b}\right)\left(\frac{MTd}{mT_b}\right)\frac{f}{d}\left(e_\mu^2 + f^2\right)g^2 - 30\left(\frac{MTd}{mT_b}\right)f - 3\left(\frac{dM}{kT_b}\right)\frac{f}{d}\left(e_\mu^2 + f^2\right)g^2 - 15f + \left(\frac{dM}{kT_b}\right)^2 f\left(e_\mu^2 + f^2\right)g^4 + 2\left(\frac{dM}{kT_b}\right)\left(\frac{MTd}{mT_b}\right)\left(e_\mu^2 + 3f^2\right)g^2 + 25\left(\frac{MTd}{mT_b}\right)^2 f - 5\left(\frac{dM}{kT_b}\right)dfg^2 - 10\left(\frac{MTd}{mT_b}\right)d + e_\mu f\left(\left(\frac{dM}{kT_b}\right)^2 fg^4 + 4\left(\frac{dM}{kT_b}\right)\left(\frac{MTd}{mT_b}\right)g^2 + 3\left(\frac{dM}{kT_b}\right)\left(\frac{MTd}{mT_b}\right)\frac{f}{d}g^2 - 3\left(\frac{dM}{kT_b}\right)\frac{f}{d}g^2\right)(1 + \cos(\chi))\right] g^5(1 - \cos(\chi))2\pi bdbdg$$

Using CCS expressions:

$$a_{21}(0) = -\frac{4}{3d} e_\mu \left(\frac{2kT_{eff}}{\mu\pi}\right)^{\frac{1}{2}} \Omega^{(1,1)} \left[e_\mu f\left(32f\frac{\Omega^{(2,3)}}{\Omega^{(1,1)}} + 16(1-d)\frac{\Omega^{(2,2)}}{\Omega^{(1,1)}} + 12(1-d)\frac{f}{d}\frac{\Omega^{(2,2)}}{\Omega^{(1,1)}} - 12\frac{f}{d}\frac{\Omega^{(2,2)}}{\Omega^{(1,1)}}\right) + 48f\left(e_\mu^2 + f^2\right)\frac{\Omega^{(1,3)}}{\Omega^{(1,1)}} + \left(12(1-d)\left(e_\mu^2 + 3f^2\right) - 18f\left(e_\mu^2 + f^2\right) - 30d^2f\right)\frac{\Omega^{(1,2)}}{\Omega^{(1,1)}} + 10d(1-d)^2 - 30(1-d)f + 15f + 25(1-d)^2f - 10(1-d)d\right]$$

Using the known ratio expression and $E^* = \frac{\Omega^{(2,3)}}{\Omega^{(2,2)}}$ and $A^* = \frac{\Omega^{(2,2)}}{\Omega^{(1,1)}}$:

$$a_{21}(0) = -\frac{4}{3d} e_\mu \left(\frac{2kT_{eff}}{\mu\pi}\right)^{\frac{1}{2}} \Omega^{(1,1)} \left[4e_\mu fA^*\left(f(8E^* - 7) + 4\left(1 - e_\mu\right)\right) - 3f\left(e_\mu^2 + f^2\right)(4B^* - 5) + 2\left(d^2(1-d) - fd(2 - 3d + 11f) + f^2(4 + 7f)\right)(6C^* - 5) + 10f\left(1 - 2e_\mu\right)^2\right]$$

Hence:

$$a_{21}^*(0) = -\frac{4}{3d}\left[\begin{array}{c} 4e_\mu fA^*\left(f(8E^* - 7) + 4\left(1 - e_\mu\right)\right) - 3f\left(e_\mu^2 + f^2\right)(4B^* - 5) + \\ 2\left(d^2(1-d) - fd(2 - 3d + 11f) + f^2(4 + 7f)\right) \\ (6C^* - 5) + 10f\left(1 - 2e_\mu\right)^2 \end{array}\right] \quad (55)$$

This matrix element contained an error in previous works by Viehland and Mason [11] that has been corrected here. The calculation for other matrix elements and their final format are given in the supplementary information. Several codes are available from the authors to calculate other matrix elements.

4. Results and discussion

While the two-temperature theory has been validated for single atoms in monoatomic gases [37,45,75–77], it has not been comprehensively studied for all-atom models and all fields until recently [1,78,79]. The reason is that there is an expectancy that the elastic collision assumption would not hold at high enough fields [8,45,80]. In short, upon a highly energetic collision between ion and gas, the expectancy is that there would be an exchange of translational energy with internal degrees of freedom (rotational and vibrational), making the collision effectively inelastic and establishing an equilibrium temperature for the ion, that one can refer to as internal temperature T_i and that could be different from the effective temperature here established. This internal temperature may be defined as the temperature at which the internal

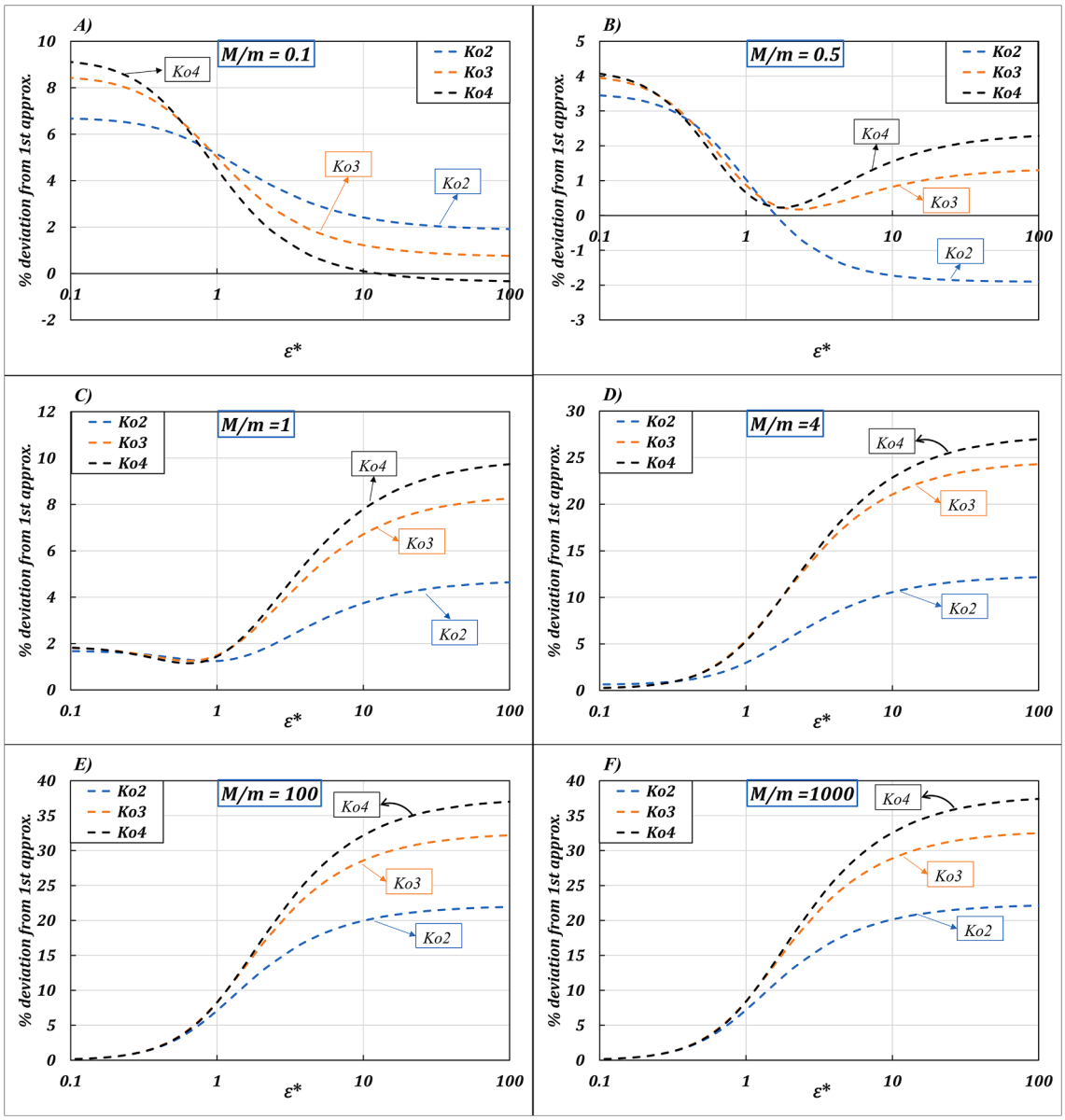

Fig. 2. The percentage difference between the first and the higher order approximations (for the hard sphere model) as a function of the dimensionless parameter $\mathscr{E}^*$ at different mass ratios (A) $M/m = 0.1$, (B) $M/m = 0.5$, (C) $M/m = 1$, (D) $M/m = 4$, (E) $M/m = 100$, (F) $M/m = 1000$. The y-axis is given by $\%\,deviation = \frac{(\langle v_d\rangle_x - \langle v_d\rangle_1)}{\langle v_d\rangle_1} \times 100$. Calculations were performed in IMoS [85].

energy difference pre- and post-collision is zero on average.

For monoatomic gases with molecular ions, once this new translational-internal equilibrium is established, the expectancy is that the collisions may be once again regarded as elastic on average, and $T_i = T_{eff}$; since the energy does not have any means of escaping the ion (neglecting radiation) other than through the translational degrees of freedom of the gas molecule [8,81]. This remains true as long as the relaxation time of the deformation caused by the ion-gas collision is smaller than the time between two consecutive collisions and the equilibrium may be established.

For molecular gases, however, the internal degrees of freedom of the gas molecule will provide means for some of the energy to escape making the collision inevitably always inelastic. Under such circumstances, it is unadvisable to use the two-temperature theory without an inelastic correction at least at moderate to high fields, and other methods are preferred [24,82]. Amongst other possibilities, although not the focus of this work, one can use the Wang–Uhlenbeck–de Boer (WUB) equation (which is an extension of the Boltzmann equation that takes into account the internal degrees of freedom). Another option is to simply assume an inelasticity or accommodation effect to describe the loss of energy [81]. This inelasticity coefficient is difficult to obtain theoretically but it can be obtained experimentally [80,83,84].

This work will therefore focus on the two-temperature theory for monoatomic gases, leaving the study of molecular gases for when sufficient data is available to study inelasticity appropriately.

4.1. Regarding the success of T_b for the two-temperature theory

The success of the two-temperature arguably relies on the choice of T_b for the base function. In general, however, one could presume that a more accurate basis function would instead include a drift velocity and an effective temperature such as:

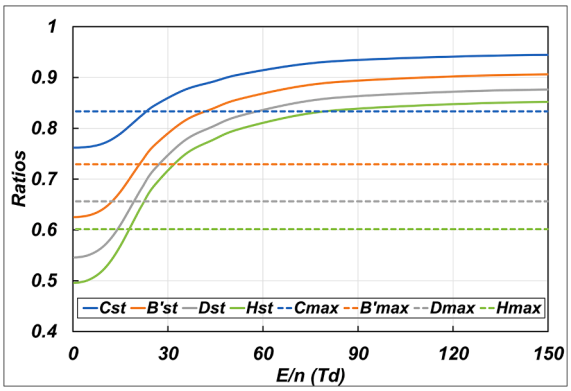

Fig. 3. CCS ratios for O^+ ion in helium gas as a function of E/n. The dashed and solid lines represent the CCS ratios for the Maxwell and 12-6-4 potential approximation model, respectively.

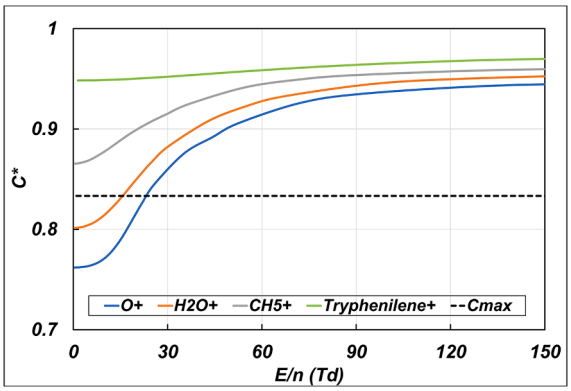

Fig. 4. C* ratios for different ions in helium gas as a function of E/n. The dashed line represents the C* ratio for the Maxwell model. The C* ratio becomes closer to 1 at low E/n as the ion size increases.

$$G^{(0)} = e^{-\frac{M(z_i - v_d)^2}{2kT_{eff}}}$$

However, the reason for the success of $F^{(0)}$ and not $G^{(0)}$ is not clear until the matrix elements are calculated. When the product of $F^{(0)}$ and f is written in terms of relative kinetic energy, the moment integrals show a distribution that can be approximated as:

$$e^{-\frac{\mu g^2}{2kT_{eff}}}(1+\phi(g))$$

where, $\phi(g)$ is a function that depends on the order of approximation. From a momentum transfer perspective, this new distribution is no different from Chapman–Enskog linearization of $G^{(0)}f$ (see A.27–28 from Larriba and Prell [9,18]). In all, since T_b includes the field energy (it relates to the ion's energy in the lab reference frame), having T_b in the basis function includes both the widening of the distribution, which is related to T_{eff}, and the translation of the distribution to the average velocity v_d, as was demonstrated by arriving at Wannier's equation for the ion's energy.

4.2. Effect of successive high field approximations for hard spheres and different mass ratios

Depending on the choice of truncation scheme for both mobility and energy, the results of the approximations may vary. Amongst the multiple options, we have opted to a) use n on the first term of the summation in Eq. (13), b) the use of Eq. (36) to calculate $\mathscr{E}$, and c) to use the same approximation is used for both mobility and energy. Finally, our scheme uses $<\psi_0^{(1)}>_i = 0$ for all approximations and not only the highest approximation. The rigid sphere case corresponds to the case where the ion is large enough that attractive ion potentials are negligible, and the physical size of the ion dominates, greatly simplifying the interaction. For a hard sphere, all the CCS ratios, e.g., C^*, A^*,…, can be substituted by 1, making the calculation extremely fast for any approximation [24], once the appropriate matrix elements are known. The results for the hard-sphere model are shown in Fig. 2 where the different approximations are compared with the first as a function of the field. For the x-axis, a dimensionless parameter is used to represent the field such as [1]:

$$\mathscr{E}^* = \left(\frac{3\pi^{1/2}}{16kT}\right)\left(\frac{m+M}{M}\right)^{1/2}\left(\frac{ze}{\pi d^2}\right)\frac{E}{n}$$

The parameter of choice, akin to $\mathscr{E}$, allows the curves to be universal despite the size of the ion d as long as the ion is spherical. The y-axis represents the deviation of successive approximations with respect to the first approximation in terms of percentage up to the fourth approximation as given by:

$$\%\ deviation = \frac{(\langle v_d\rangle_x - \langle v_d\rangle_I)\ \times\ 100}{\langle v_d\rangle_I},$$

where, x represents the order of approximation. The first approximation is therefore the x-axis and the difference between the other approximations with respect to the first is given by K_{ox}. As the matrix elements depend on the masses of both ion and gas, the results are shown for different mass ratios. It is interesting to see the variation from $M/m < 1$ to $M/m > 1$. For low mass ratios, the variation from the first approximation is largest at low fields. The opposite occurs for high mass ratios where the largest variation occurs at high fields. Two types of convergence can be observed. As $M/m \to \infty$ the deviation seems to reach an asymptote as there is little difference between the 100 and 1000 cases. In terms of overall convergence, the difference in the deviation between successive approximations seems to become smaller with higher approximations. For this reason, and the fact that the ions of interest in ion mobility and analytical chemistry follow ratios $M/m > 1$ and $\mathscr{E}^* \leq 10$, one can conclude that the 4th approximation should be sufficient to achieve acceptable results for all fields. It is important to mention that our results, although qualitatively similar, vary from those of Viehland and Mason [11].

4.3. The Maxwell Model and collision cross section ratios

One of the most important criteria for truncation schemes used in the two-temperature theory relies on the assumption that a general solution for an ion gas pair will be similar to that of the Maxwell Model (a r^{-4} interaction) [10]. The Maxwell Model was initially proposed for vanishing fields ($E/n \to 0$) for the one-temperature theory where off-diagonal coefficients of the matrix elements are zero [25]. For the two-temperature theory, it has been stated that off-diagonal terms do survive although only those where $s \leq r$. It is therefore important to study how molecular ions with a physical size and a 12-6-4 potential interaction evolve in comparison to the Maxwell model. This is preferably done in terms of ratios of collision cross sections as their value is well known for the Maxwell model. A particularity of the Maxwell model is that the $Q^{(l)}$ integral is proportional to $1/g$ which can be used to obtain the ratios. For example, for C^*, B^* or A^* for the Maxwell model:

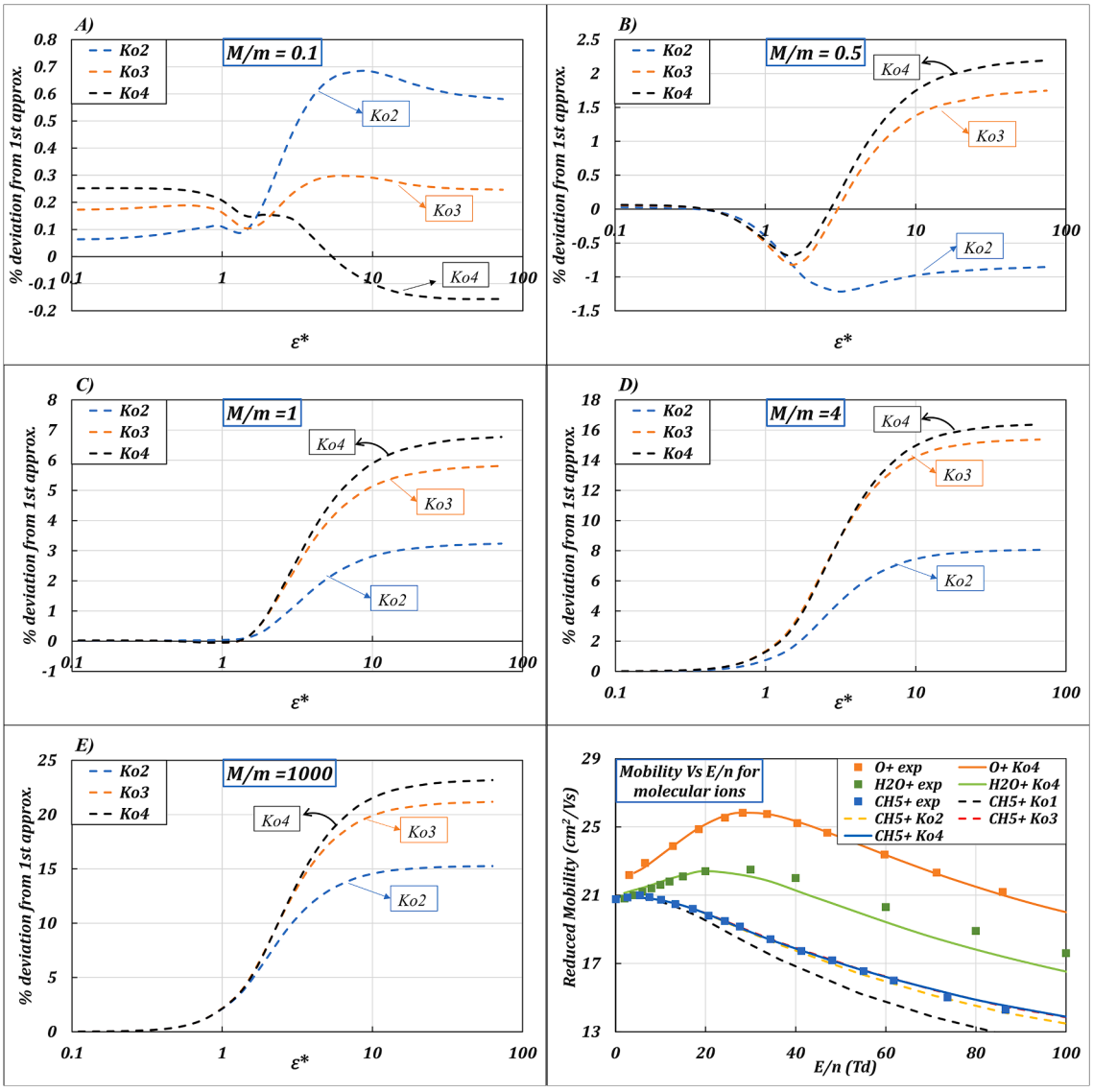

Fig. 5. The percentage difference between the first and the higher order approximations (using the 12-6-4 Lennard-Jones trajectory method) as a function of the dimensionless parameter ε^* at different mass ratios (A) $M/m = 0.1$, (B) $M/m = 0.5$, (C) $M/m = 1$, (D) $M/m = 4$, (E) $M/m = 1000$. The y-axis is given by $\%\,deviation = \frac{(\langle v_d \rangle_x - \langle v_d \rangle_1)}{\langle v_d \rangle_1} \times 100$. Fig. 5F shows the experimental and the calculated mobility for O^+, H_2O^+ and CH_5^+ in helium as a function of E/n. For CH_5^+, the mobility using different approximations is illustrated. Calculations were performed in IMoS [85].

$$C^* = \frac{\Omega^{(1,2)}(T_{eff})}{\Omega^{(1,1)}(T_{eff})} = \frac{\frac{2}{(3)!}\left(\frac{\mu}{2kT_{eff}}\right)^4 \int_0^\infty e^{-\left(\frac{\mu}{2kT_{eff}}\right)g^2} g^7 Q^{(1)}(g)dg}{\frac{2}{(2)!}\left(\frac{\mu}{2kT_{eff}}\right)^3 \int_0^\infty e^{-\left(\frac{\mu}{2kT_{eff}}\right)g^2} g^5 Q^{(1)}(g)dg} = \frac{\frac{2}{(3)!}\left(\frac{\mu}{2kT_{eff}}\right)^4 \int_0^\infty e^{-\left(\frac{\mu}{2kT_{eff}}\right)g^2} g^6 Q^{*(1)}dg}{\frac{2}{(2)!}\left(\frac{\mu}{2kT_{eff}}\right)^3 \int_0^\infty e^{-\left(\frac{\mu}{2kT_{eff}}\right)g^2} g^4 Q^{*(1)}dg} = \frac{5}{6} \tag{56}$$

$$B^* = 5C^* - 4\frac{\Omega^{(1,3)}(T_{eff})}{\Omega^{(1,1)}(T_{eff})} = 5C^* - 4\frac{\frac{2}{(4)!}\left(\frac{\mu}{2kT_{eff}}\right)^5 \int_0^\infty e^{-\left(\frac{\mu}{2kT_{eff}}\right)g^2} g^8 Q^{*(1)}dg}{\frac{2}{(2)!}\left(\frac{\mu}{2kT_{eff}}\right)^3 \int_0^\infty e^{-\left(\frac{\mu}{2kT_{eff}}\right)g^2} g^4 Q^{*(1)}dg} = 5C^* - 4B'^* = 5\frac{5}{6} - \frac{35}{48} = \frac{5}{4} \tag{57}$$

$$A^* = \frac{\Omega^{(2,2)}(T_{eff})}{\Omega^{(1,1)}(T_{eff})} = \frac{\frac{2}{(3)!}\left(\frac{\mu}{2kT_{eff}}\right)^4 \int_0^\infty e^{-\left(\frac{\mu}{2kT_{eff}}\right)g^2} g^7 Q^{(2)}(g)dg}{\frac{2}{(2)!}\left(\frac{\mu}{2kT_{eff}}\right)^3 \int_0^\infty e^{-\left(\frac{\mu}{2kT_{eff}}\right)g^2} g^5 Q^{(1)}(g)dg} = \frac{\frac{2}{(3)!}\left(\frac{\mu}{2kT_{eff}}\right)^4 \int_0^\infty e^{-\left(\frac{\mu}{2kT_{eff}}\right)g^2} g^6 Q^{*(2)}dg}{\frac{2}{(2)!}\left(\frac{\mu}{2kT_{eff}}\right)^3 \int_0^\infty e^{-\left(\frac{\mu}{2kT_{eff}}\right)g^2} g^4 Q^{*(1)}dg} = \frac{5Q^{*(2)}}{6Q^{*(1)}} \tag{58}$$

where, $Q^{*(l)} = gQ^{(l)}$ and independent of g. The rest of the ratios can be equally calculated and are provided in the supplementary information. The ratios $A^* = \frac{\Omega^{(2,2)}(T_{eff})}{\Omega^{(1,1)}(T_{eff})}$ and $F^* = \frac{\Omega^{(3,3)}(T_{eff})}{\Omega^{(1,1)}(T_{eff})}$ are ratios whose numerical values depend on the angular pattern (see Eq. (56)) while the rest of the ratios have established values.

The general expressions for the matrix elements $a^*_{rs}(l)$ can then be written following the expectancy that general ratios are close to Maxwell model ratios results. It is then easy to see why those matrix elements with $s > r$ are zero for the Maxwell model (as advanced previously). For one of the examples above, $a^*_{02}(1) = -\frac{8d^2}{105}[3(4B^* - 5) + 4(6C^* - 5)]$, in which $s > r$, the matrix element will be zero for the Maxwell model. Elements with $s \leq r$ always have a nonzero extra term, e.g., $10f(1 - 2e_\mu)^2$ for $a^*_{21}(0)$.

It would be interesting to study the deviation from the expected Maxwellian values of the ratios for small ions in He gas. The results for a few of the ratios are shown in Fig. 3 for O^+ with a 12-6-4 potential. Very noticeable is that all ratios follow a similar tendency. They start below the Maxwell assumption and increase asymptotically to 1 as E/n increases. At the low field, the oxygen ion acts very similarly to how a 4-interaction potential would, with an additional effect from the 6-interaction potential. As the field increases, the ion starts acting more like a hard sphere due to the 12-interaction potential that becomes dominant. As such the CCS ratios become close to 1 the higher the field interaction is [13]. In all, note that for low fields, 0-40Td, substitution of the ratios for their Maxwell value is a decent approximation for monoatomic ions as shown by Mason and McDaniel [16]. As the ion becomes larger, however, the 4-6 interaction effect should become weaker compared to the effect of the physical size (or 12-interaction) even at lower fields. This can be observed for C^* in Fig. 4 for ions of increasing size, namely O^+, H_2O^+, CH_5^+ and Tryphenilene. The larger the ion, the closer to 1 the ratios are and the further away from the Maxwell effect. It is therefore not recommended to use Maxwell ratios for molecular ions and perform the actual calculations.

4.4. Calculations for small ions and spherical gases for arbitrary fields

An ideal situation for the two-temperature theory is that of two monoatomic entities, ion and gas interacting together. Under such circumstances, the collisions may be regarded as fully elastic, and the theory should be able to describe the collision quite accurately in the instances where quantum effects may be regarded as negligible [8,13,86]. For such cases, a 12-6-4 interaction potential between two monoatomic entities combines the most important long-range effects as well as the repulsion core. The r^{-4} corresponds to the ion-induced dipole attraction while the 6-12 is a simplified, numerically optimized intermolecular interaction termed the Lennard-Jones potential, which represents the combination of the induced-dipole/induced-dipole attraction (r^{-6}) and the electron cloud repulsion (r^{-12}). This interaction is typically expected to be quite accurate for all fields as long as the Lennard-Jones parameters, well-depth and zero potential energy crossing (ϵ *and* σ), are optimized. Given that the matrix elements heavily depend on the mass, one would also like to compare the different possible approximations, and their effect for different mass ratios and different potential interactions. Fig. 5 A–E shows the results of the difference between mobility approximations (akin to Fig. 2) for an oxygen atom with a 12-6-4 potential interaction and for different ion-to-gas mass ratios. The Lennard-Jones potentials for Oxygen used were $\sigma = 3.043$Å and $\epsilon = 0.214668\ e^{-21}J$. These results are expected to vary from the hard sphere ones in particular for smaller mass ratios, while for larger mass ratios the values are expected to be qualitatively similar.

One would like to test the results of the two-temperature theory for small ions in light gases with respect to experiments. This is shown in Fig. 5F, where the reduced mobility of O^+, H_2O^+ and CH_5^+ are shown as a function of E/n both numerically (4th approximation) using IMoS [85,87] and experimentally in He [23,56]. The program is available and free of charge (www.imospedia.com) and uses a parallelized interface to calculate reduced mobilities and CCS for different gases. Similar results for a variety of small ions are shown in a companion paper to this one [1]. It is clear that for the monoatomic ion, the two-temperature theory reproduces the experimental results quite accurately. For the polyatomic ions, the theoretical results follow the experimental curves quite well (given that the experimental results have a 7% error). Finally, for CH_5^+, all approximations are shown (one through four). Given that the mass ratio is about 4, it is expected that the largest differences between the approximations will occur at high fields. This is visibly the case in Fig. 5F. The higher the approximation the closer the result is to the experimental values. One can also observe that the difference between the third and fourth approximation is rather small, hinting towards convergence.

5. Limitations of the two-temperature theory

The two-temperature theory has demonstrated its validity in predicting ion mobility for monoatomic gases, but its viability for molecular gases remains uncertain. As advanced in the introduction, this uncertainty stems from the idea that as the ion increases its kinetic energy, its collisions with the gas will no longer be translationally elastic, breaking the elasticity assumption established in the two-temperature theory. This is a topic of ongoing research since 1983, when Larry Viehland conducted a series of experiments and obtained different values of effective temperatures theoretically and experimentally for a given mobility, thereby confirming the concept. The energy loss from inelastic collisions was condensed into the "inelasticity parameter (ξ)" which can be calculated by the equation [80]:

$$\xi = \frac{M}{m}\left(\frac{T_{eff}^{el}}{T_{eff}^{inel}} - 1\right) \tag{59}$$

where, T_{eff}^{inel} represents experimental effective temperature and T_{eff}^{el} represents the two-temperature theory effective temperature for a given mobility. In general, this inelastic parameter should be very small for small molecular ions in monoatomic gases, as after an equilibrium effective temperature is reached in the internal degrees of freedom, there are no other modes of escape for the translational energy, and it becomes effectively elastic again. This has been proven previously for He [1,88]. However, if the molecular ion is sufficiently large, the effective equilibrium temperature might not be reached. The effect should be even more noticeable for molecular ions in monoatomic gases. In such a case, even if an effective temperature is reached internally in the molecular ion, there is always a mode of energy escape through the internal and rotational degrees of freedom of the gas molecule. Therefore, the expectancy is that inelasticity effects will be present for any ion in molecular gases under sufficiently high fields. For small to medium fields, the effect can be most likely neglected [89]. The theory to study the effects of internal degrees of freedom exists through the WUB equation. However, due to its complexity, its use is precluded for molecular ions at least for now and initial data must be obtained through experimental to theory comparison.

Given the lack of internal and rotational degrees of freedom in the Boltzmann equation for the two-temperature theory, another limitation is that any mobility differentiation due purely to rotational and vibrational degrees of freedom may not be obtained. One such case has been that of isotopomers (same structure and same mass, but different location of isotopic substitutions) [5–7], where it has recently been shown that they are separable by ion mobility due to shifts in their centre of mass and moment of inertia.

6. Conclusions

This manuscript aims to provide a concise description of the two-temperature theory along with rigorous mathematical arguments behind its success at predicting the ion's drift velocity in monoatomic gases at high fields. Moreover, a thorough procedure for obtaining the equations (including the matrix elements) for higher-order mobility approximations is also provided with high detail, making this work suitable for beginners and experts in ion mobility. The work itself tries to explain the suitability of the two-temperature theory with concrete arguments of why the theory works and when it should be employed. The key takeaways of the manuscript can be consolidated as below:

- The success of the two-temperature theory relies on the choice of a basis function with a base temperature (T_b) related to the ion's temperature and different from the gas temperature (T). The base temperature starts as a parameter, but a relation between the temperature and the field over the concentration must be made at some point.
- Different moments of the Boltzmann equation need to be solved to determine various transport properties, e.g., drift velocity (v_d), energy, etc. The solution assumes that the collision operator may be written in terms of an infinite sum of orthogonal functions (Burnett) with coefficients that are known as matrix elements. Since the moments cannot be obtained without knowing the ion's velocity distribution a priori, a recursive relation is sought, for which different approximations can be obtained from lower-order approximations, starting with the first.
- Different successive approximations are dependant on complicated functions of the matrix elements. The matrix elements themselves are as well complicated functions of ratios of Collision Integrals. The explanation of how to calculate these matrix elements has been thoroughly explained in this manuscript, for the first time to our knowledge. Full results are shown up to the third approximation, while numerically, up to the fourth approximation is calculated in IMoS. The expressions are written such that the off-diagonal terms get cancelled if the Maxwell model is used.
- A choice needs to be made for the base temperature. If the $3/2kT_b$ is chosen to be equivalent to the ion's energy, a relation may be calculated that relates T_b to E/n to different approximations, leading to a closed-form equation of the ion mobility. The method chosen here can accurately solve higher-order mobility equations almost instantaneously once the collision integrals are calculated, in contrast to other methods, which might take several minutes or hours.
- The first approximation of the ion's energy yields Wannier's energy equation. This establishes that $3/2kT_b$ can be related to the kinetic energy of the ion due to the field plus the translational energy at a temperature higher than that of the gas, due to collisional heating, and that it is labelled the effective temperature T_{eff}.
- The effect of higher-order approximations was tested for different M/m ratios first for the hard sphere case and then for a 12-6-4 potential. Interestingly, in all cases, the deviation in mobility between successive approximations was reduced, indicating convergence. Moreover, the two-temperature theory has been tested for monoatomic and polyatomic ions in Helium gas at high E/n showing excellent correlation with experimental results, further solidifying the hypothesis.
- Several collision integral ratios of different ions (using a 12-6-4 potential) were calculated as a function of E/n. For monoatomic and small polyatomic ions, the ratios were found to be similar to those of the Maxwell model at moderate fields (0-40 Td), and similar to those for of the hard-sphere model at high fields (i.e., approaching asymptotically at 1). For monoatomic or very small polyatomic ions, substituting the ratios for their Maxwell values may therefore yield acceptable results at low fields. However, it is not practical to utilize the Maxwell model for bigger polyatomic ions because the ratios deviate even at negligible fields.
- For polyatomic ions in high E/n, it is expected for collisions to be inelastic in the translational sense, meaning that some of the collisional energy is transferred to the internal degrees of freedom of both ion and gas molecule. For monoatomic gases, the inelasticity can be generally ignored because there is no mode of energy escape once the ion's internal energy reaches equilibrium with the relative translational energy of collision, and the two-temperature theory stays valid. For polyatomic gases, however, some of the energy can always escape the system through the internal degrees of freedom of the gas, making the two-temperature theory less accurate with increasing fields.

Funding sources

Carlos Larriba-Andaluz would like to acknowledge that this work was supported by CMI NSF under Grant 1904879 and Grant 2203968. Xuemeng Chen would like to acknowledge EU's Horizon 2020 research and innovation programme–Marie Skłodowska-Curie grant No 896914.

Declaration of Competing Interest

All authors declare that they have no conflict of interest.

Data availability

Data will be made available on request.

Supplementary materials

Supplementary material associated with this article can be found, in the online version, at doi:10.1016/j.talo.2023.100191.

References

[1] V.D. Gandhi, C. Larriba-Andaluz, Predicting ion mobility as a function of the electric field for small ions in light gases, Anal. Chim. Acta 1184 (2021), 339019.
[2] F. Lanucara, S.W. Holman, C.J. Gray, C.E. Eyers, The power of ion mobility-mass spectrometry for structural characterization and the study of conformational dynamics, Nat. Chem. 6 (4) (2014) 281–294.
[3] I. Campuzano, M.F. Bush, C.V. Robinson, C. Beaumont, K. Richardson, H. Kim, H. I. Kim, Structural characterization of drug-like compounds by ion mobility mass spectrometry: comparison of theoretical and experimentally derived nitrogen collision cross sections, Anal. Chem. 84 (2) (2012) 1026–1033.
[4] J.W. Lee, H.H.L. Lee, K.L. Davidson, M.F. Bush, H.I. Kim, Structural characterization of small molecular ions by ion mobility mass spectrometry in nitrogen drift gas: improving the accuracy of trajectory method calculations, Analyst 143 (8) (2018) 1786–1796.
[5] C.P. Harrilal, V.D. Gandhi, G. Nagy, X. Chen, M.G. Buchanan, R. Wojcik, C. R. Conant, M.T. Donor, Y.M. Ibrahim, S.V. Garimella, Measurement and theory of gas-phase ion mobility shifts resulting from isotopomer mass distribution changes, Anal. Chem. 93 (45) (2021) 14966–14975.
[6] J.L. Kaszycki, A.P. Bowman, A.A. Shvartsburg, Ion mobility separation of peptide isotopomers, J. Am. Soc. Mass Spectrom. 27 (5) (2016) 795–799.
[7] R. Wojcik, G. Nagy, I.K. Attah, I.K. Webb, S.V. Garimella, K.K. Weitz, A. Hollerbach, M.E. Monroe, M.R. Ligare, F.F. Nielson, SLIM ultrahigh resolution ion mobility spectrometry separations of isotopologues and isotopomers reveal mobility shifts due to mass distribution changes, Anal. Chem. 91 (18) (2019) 11952–11962.
[8] C. Larriba-Andaluz, A perspective on the theoretical and numerical aspects of ion mobility spectrometry, Int. J. Mass Spectrom. 470 (2021), 116719.
[9] C. Larriba-Andaluz, J.S. Prell, Fundamentals of ion mobility in the free molecular regime. Interlacing the past, present and future of ion mobility calculations, Int. Rev. Phys. Chem. 39 (4) (2020) 569–623.
[10] L.A. Viehland, E. Mason, Gaseous lon mobility in electric fields of arbitrary strength, Ann. Phys. (N. Y.) 91 (2) (1975) 499–533.
[11] L.A. Viehland, E. Mason, Gaseous ion mobility and diffusion in electric fields of arbitrary strength, Ann. Phys. (N. Y.) 110 (2) (1978) 287–328.
[12] T. Kihara, The mathematical theory of electrical discharges in gases. B. Velocity-distribution of positive ions in a static field, Rev. Mod. Phys. 25 (4) (1953) 844.
[13] E.W. McDaniel, E.A. Mason. Mobility and diffusion of ions in gases, Wiley Series in Plasma Physics, John Wiley & Sons, New York, 1973.
[14] E. Krylov, E. Nazarov, Electric field dependence of the ion mobility, Int. J. Mass Spectrom. 285 (3) (2009) 149–156.
[15] I. Buryakov, E. Krylov, E. Nazarov, U.K. Rasulev, A new method of separation of multi-atomic ions by mobility at atmospheric pressure using a high-frequency amplitude-asymmetric strong electric field, Int. J. Mass Spectrom. Ion Process. 128 (3) (1993) 143–148.
[16] E.A. Mason, E.W. McDaniel. Transport properties of ions in gases, John Wiley & Sons, New York, 1988.
[17] E.W. McDaniel, L. Viehland, The transport of slow ions in gases: experiment, theory, and applications, Phys. Rep. 110 (5–6) (1984) 333–367.
[18] S. Chapman, T.G. Cowling, The Mathematical Theory of Non-Uniform gases: An Account of the Kinetic Theory of Viscosity, Thermal Conduction and Diffusion in Gases, Cambridge University Press, 1990.
[19] J. Whealton, E. Mason, Transport coefficlents of gaseous ions in an electric field, Ann. Phys. (N. Y.) 84 (1–2) (1974) 8–38.
[20] L.A. Viehland, S. Lin, Application of the three-temperatue theory of gaseous ion transport, Chem. Phys. 43 (1) (1979) 135–144.
[21] S. Lin, L. Viehland, E. Mason, Three-temperature theory of gaseous ion transport, Chem. Phys. 37 (3) (1979) 411–424.
[22] L.A. Viehland, Velocity distribution functions and transport coefficients of atomic ions in atomic gases by a Gram–Charlier approach, Chem. Phys. 179 (1) (1994) 71–92.
[23] H. Ellis, R. Pai, E. McDaniel, E. Mason, L. Viehland, Transport properties of gaseous ions over a wide energy range, Atomic Data Nuclear Data Tables 17 (3) (1976) 177–210.
[24] L.A. Viehland, Gaseous Ion mobility, diffusion, and Reaction, Springer, 2018.
[25] E.A. Mason, H.W. Schamp Jr, Mobility of gaseous lons in weak electric fields, Ann. Phys. (N. Y.) 4 (3) (1958) 233–270.
[26] J. Aisbett, J.M. Blatt, A.H. Opie, General calculation of the collision integral for the linearized Boltzmann transport equation, J. Stat. Phys. 11 (6) (1974) 441–456.
[27] D. Spalding, The molecular theory of gases and liquids, Diagrams. 160s,, Aeronaut. J. 59 (531) (1955) 228, 228.
[28] M. Abramowitz, I.A. Stegun, Handbook of Mathematical Functions, Dover Publications, New York, 1965, p. 361.
[29] P. Panat, B. Paranjape, R. Teshima, A simple theory of mobility for ions in gases, J. Phys. D Appl. Phys. 16 (8) (1983) 1477.
[30] K. Suchy, Neue Methoden in Der Kinetischen Theorie verdünnter Gase, Ergebnisse der Exakten Naturwissenschaften, Springer, 1964, pp. 103–294.
[31] F. Weitzsch, Ein neuer Ansatz für die Behandlung gasdynamischer Probleme bei starken Abweichungen vom Thermodynamischen Gleichgewicht, Ann. Phys. 462 (7–8) (1961) 403–417.
[32] H. Skullerud, Kinetic Theory of Ion Transport in gases, Electrical Breakdown and Discharges in Gases, Springer, 1983, pp. 177–186.
[33] P. Almeida, M. Benilov, G. Naidis, Calculation of ion mobilities by means of the two-temperature displaced-distribution theory, J. Phys. D Appl. Phys. 35 (13) (2002) 1577.
[34] S. Lin, J. Bardsley, Monte Carlo simulation of ion motion in drift tubes, J. Chem. Phys. 66 (2) (1977) 435–445.
[35] C. Cercignani, Mathematical Methods in Kinetic Theory, Springer, 1969.
[36] D. Burnett, The distribution of velocities in a slightly non-uniform gas, Proc. Lond. Math. Soc. 2 (1) (1935) 385–430.
[37] I. Gatland, L. Viehland, E. Mason, Tests of alkali ion-inert gas interaction potentials by gaseous ion mobility experiments, J. Chem. Phys. 66 (2) (1977) 537–541.
[38] L. Viehland, Internal-energy distribution of molecular ions in drift tubes. Swarms of Ions and Electrons in Gases, Springer, 1984, pp. 27–43.
[39] G.H. Wannier, Motion of gaseous ions in strong electric fields, Bell Syst. Tech. J. 32 (1) (1953) 170–254.
[40] H. Skullerud, Monte-Carlo investigations of the motion of gaseous ions in electrostatic fields, J. Phys. B Atomic and Mol. Phys. (1968–1987) 6 (4) (1973) 728.
[41] G.H. Wannier, On the motion of gaseous ions in a strong electric field. I, Phys. Rev. 83 (2) (1951) 281.
[42] G.H. Wannier, Motion of gaseous ions in a strong electric field. II, Phys. Rev. 87 (5) (1952) 795.
[43] B.M. Smirnov, Mobility of heavy ions in gas, Doklady Akademii Nauk, Russ. Acad. Sci. (11) (1966) 322–324.
[44] G.E. Spangler, R.A. Miller, Application of mobility theory to the interpretation of data generated by linear and RF excited ion mobility spectrometers, Int. J. Mass Spectrom. 214 (1) (2002) 95–104.
[45] L. Viehland, S. Lin, E. Mason, Kinetic theory of drift-tube experiments with polyatomic species, Chem. Phys. 54 (3) (1981) 341–364.
[46] M. Waldman, E. Mason, Generalized Einstein relations from a three-temperature theory of gaseous ion transport, Chem. Phys. 58 (1) (1981) 121–144.
[47] P. Ong, M.M. Li, Monte Carlo simulation studies on the validity of the Gram-Charlier calculations of velocity distributions of Na^+ swarm in neon gas, Chem. Phys. 211 (1–3) (1996) 115–122.
[48] L.A. Viehland, E. Mason, Statistical–mechanical theory of gaseous ion–molecule reactions in an electrostatic field, J. Chem. Phys. 66 (2) (1977) 422–434.
[49] E. Mason, H.S. Hahn, Ion drift velocities in gaseous mixtures at arbitrary field strengths, Phys. Rev. A 5 (1) (1972) 438.
[50] J. Whealton, E. Mason, Composition dependence of ion diffusion coefficients in gas mixtures at arbitrary field strengths, Phys. Rev. A 6 (5) (1972) 1939.
[51] J. Whealton, E. Mason, R. Robson, Composition dependence of ion-transport coefficients in gas mixtures, Phys. Rev. A 9 (2) (1974) 1017.
[52] H.B. Milloy, R.E. Robson, The mobility of potassium ions in gas mixtures, J. Phys. B Atomic Mol. Phys. (1968–1987) 6 (6) (1973) 1139.
[53] H.S. Hahn, E. Mason, Energy partitioning of gaseous ions in an electric field, Phys. Rev. A 7 (4) (1973) 1407.
[54] H.M. Rosenstock, K. Draxl, B. Steiner, J.T. Herron, Energetics of Gaseous Ions, National Standard Reference Data System, 1977.
[55] H. Ellis, M. THACKSTON, E. McDaniel, E. Mason, Transport properties of gaseous ions over a wide energy range. Part III, Atomic Data Nuclear Data Tables 31 (1984) 113.
[56] H. Ellis, E. McDaniel, D. Albritton, L. Viehland, S. Lin, E. Mason, Transport properties of gaseous ions over a wide energy range. Part II, Atomic Data Nuclear Data Tables 22 (3) (1978) 179–217.
[57] H. Wilhelm, Kinetic theory of subsonic and supersonic transport processes in weakly ionized gases, Il Nuovo Cimento B (1965–1970) 68 (2) (1970) 189–207.
[58] H. Dreicer, Electron and ion runaway in a fully ionized gas. I, Phys. Rev. 115 (2) (1959) 238.
[59] H. Dreicer, Electron and ion runaway in a fully ionized gas. II, Phys. Rev. 117 (2) (1960) 329.
[60] D. Morsa, V. Gabelica, E. De Pauw, Effective temperature of ions in traveling wave ion mobility spectrometry, Anal. Chem. 83 (14) (2011) 5775–5782.
[61] X. An, G.A. Eiceman, R.M. Räsänen, J.E. Rodriguez, J.A. Stone, Dissociation of proton bound ketone dimers in asymmetric electric fields with differential mobility spectrometry and in uniform electric fields with linear ion mobility spectrometry, J. Phys. Chem. A 117 (30) (2013) 6389–6401.
[62] A.A. Shvartsburg, R.D. Smith, A. Wilks, A. Koehl, D. Ruiz-Alonso, B. Boyle. Differential ion mobility spectrometry: nonlinear ion transport and fundamentals of FAIMS, CRC Press, Boca Raton, FL, 2008.
[63] S. Lee, T. Wyttenbach, M.T. Bowers, Gas phase structures of sodiated oligosaccharides by ion mobility/ion chromatography methods, Int. J. Mass Spectrom. Ion Process. 167 (1997) 605–614.
[64] J.T. Hopper, N.J. Oldham, Collision induced unfolding of protein ions in the gas phase studied by ion mobility-mass spectrometry: the effect of ligand binding on conformational stability, J. Am. Soc. Mass Spectrom. 20 (10) (2009) 1851–1858.
[65] C. Bleiholder, F.C. Liu, M. Chai, Comment on effective temperature and structural rearrangement in trapped ion mobility spectrometry, Anal. Chem. 92 (24) (2020) 16329–16333.
[66] C. Schaefer, A.T. Kirk, M. Allers, S. Zimmermann, Ion mobility shift of isotopologues in a high kinetic energy ion mobility spectrometer (HiKE-IMS) at elevated effective temperatures, J. Am. Soc. Mass Spectrom. 31 (10) (2020) 2093–2101.

[67] A.V. Tolmachev, A.N. Vilkov, B. Bogdanov, L. PĂsa-Tolić, C.D. Masselon, R. D. Smith, Collisional activation of ions in RF ion traps and ion guides: the effective ion temperature treatment, J. Am. Soc. Mass Spectrom. 15 (11) (2004) 1616–1628.
[68] G. Ford, Matrix elements of the linearized collision operator, Phys. Fluids 11 (3) (1968) 515–521.
[69] B. Shizgal, J. Fitzpatrick, Matrix elements of the linear Boltzmann collision operator for systems of two components at different temperatures, Chem. Phys. 6 (1) (1974) 54–65.
[70] M.J. Lindenfield, B. Shizgal, Matrix elements of the Boltzmann collision operator for gas mixtures, Chem. Phys. 41 (1–2) (1979) 81–95.
[71] S. Lin, R. Robson, E. Mason, Moment theory of electron drift and diffusion in neutral gases in an electrostatic field, J. Chem. Phys. 71 (8) (1979) 3483–3498.
[72] J.A. Hornbeck, The drift velocities of molecular and atomic ions in helium, neon, and argon, Phys. Rev. 84 (4) (1951) 615.
[73] C. Chang, G. Meisels, J. Taylor, High-pressure mass spectrometry: ion energies and their distributions in chemical ionization sources, Int. J. Mass Spectrom. Ion Phys. 12 (5) (1973) 411–421.
[74] W. Vincenti, C. Kruger. Introduction to physical gas dynamics, Wiley, New York, 1965.
[75] G.R. Freeman, D.A. Armstrong, Electron and Ion Mobilities, Advances in Atomic and Molecular Physics, Elsevier, 1985, pp. 267–325.
[76] I. Gatland, W. Morrison, H. Ellis, M. Thackston, E. McDaniel, M. Alexander, L. Viehland, E. Mason, The Li^+–He interaction potential, J. Chem. Phys. 66 (11) (1977) 5121–5125.
[77] D. Lamm, M. Thackston, F. Eisele, H. Ellis, J. Twist, W. Pope, I. Gatland, E. McDaniel, Mobilities and interaction potentials for K^+–Ar, K^+–Kr, and K^+–Xe, J. Chem. Phys. 74 (5) (1981) 3042–3045.
[78] S. Dubrovskii, N. Balabaev, Simulation of the drift of a macromolecular ion in a gas under the action of an electric field, Polym. Sci. Ser. A 63 (6) (2021) 891–901.
[79] S. Dubrovskii, N. Balabaev, Molecular dynamics simulation of the behavior of protonated poly (ethylene oxide) s in drift tube experiments, Polym. Sci. Ser. A 64 (2022) 1–10.
[80] L. Viehland, D. Fahey, The mobilities of NO− 3, NO− 2, NO^+, and Cl^- in N_2: a measure of inelastic energy loss, J. Chem. Phys. 78 (1) (1983) 435–441.
[81] G.E. Uhlenbeck, J. De Boer. Studies in statistical mechanics, Interscience, New York, 1962.
[82] W. Federer, H. Ramler, H. Villinger, W. Lindinger, Vibrational temperature of O^{2+} and N^{2+} drifting at elevated E N in Helium, Phys. Rev. Lett. 54 (6) (1985) 540.
[83] G. Eiceman, Z. Karpas, Ion Mobility Spectrom, Taylor & Francis, New York, 2005.
[84] Y. Kaneko, L. Megill, J. Hasted, Study of inelastic collisions by drifting ions, J. Chem. Phys. 45 (10) (1966) 3741–3751.
[85] V.D. Gandhi, K. Short, L. Hua, I. Rodríguez, C. Larriba-Andaluz, A numerical tool to calculate ion mobility at arbitrary fields from all-atom models, J. Aerosol. Sci. (2022), 106122.
[86] S.A. McLuckey, Principles of collisional activation in analytical mass spectrometry, J. Am. Soc. Mass Spectrom. 3 (6) (1992) 599–614.
[87] V. Shrivastav, M. Nahin, C.J. Hogan, C. Larriba-Andaluz, Benchmark comparison for a multi-processing ion mobility calculator in the free molecular regime, J. Am. Soc. Mass Spectrom. 28 (8) (2017) 1540–1551.
[88] V. Gabelica, E. Marklund, Fundamentals of ion mobility spectrometry, Curr. Opin. Chem. Biol. 42 (2018) 51–59.
[89] A. Wilks, M. Hart, A. Koehl, J. Somerville, B. Boyle, D. Ruiz-Alonso, Characterization of a miniature, ultra-high-field, ion mobility spectrometer, Int. J. Ion Mob. Spectrom. 15 (3) (2012) 199–222.